Simulating human impacts on global water resources using VIC-5

Bram Droppers[1], Wietse H.P. Franssen[1], Michelle T.H. van Vliet[2], Bart Nijssen[3], Fulco Ludwig[1]

[1] Water Systems and Global Change Group, Department of Environmental Sciences, Wageningen University, Wageningen, 6708 PB, The Netherlands
[2] Department of Physical Geography, Utrecht University, Utrecht, 3584 CS, The Netherlands
[3] Computational Hydrology Group, Department of Civil and Environmental Engineering, University of Washington, Seattle, 98195, United States of America

Correspondence to: Bram Droppers (bram.droppers@wur.nl)

Abstract. Questions related to historical and future water resources and scarcity have been addressed by several macro-scale hydrological models. One of these models is the Variable Infiltration Capacity (VIC) model. However, further model developments were needed to holistically assess anthropogenic impacts on global water resources using VIC.

Our study developed VIC-WUR, which extends the VIC model with: (1) integrated routing, (2) surface and groundwater use for various sectors (irrigation, domestic, industrial, energy and livestock), (3) environmental flow requirements for both surface and groundwater systems, and (4) dam operation. Global gridded datasets on sectoral demands were developed separately and used as an input to the VIC-WUR model.

Simulated national water withdrawals were in line with reported FAO national annual withdrawals (R^2 adjusted > 0.8), both per sector as well as per source. However, trends in time for domestic and industrial water withdrawal were mixed compared to other previous studies. GRACE monthly terrestrial water storage anomalies were well represented (global mean RMSE of 1.9 and 3.5 for annual and interannual anomalies respectively), while groundwater depletion trends were overestimated. The implemented human impact modules increased simulated streamflow performance for 370 out of 462 human-impacted GRDC monitoring stations, mostly due to the effects of reservoir operation. An assessment of environmental flow requirements indicates that global water withdrawals have to be severely limited (by 39 %) to protect aquatic ecosystems, especially for groundwater withdrawals.

VIC-WUR has potential for studying impacts of climate change and anthropogenic developments on current and future water resources and sectoral specific-water scarcity. The additions presented here make the VIC model more suited for fully-integrated worldwide water-resource assessments.

1 Introduction

Questions related to historical and future water resources and scarcity have been addressed by several macro-scale hydrological models over the last few decades (Liang et al., 1994; Alcamo et al., 1997; Hagemann and Gates, 2001; Takata et al., 2003; Krinner et al., 2005; Bondeau et al., 2007; Hanasaki et al., 2008b; Van Beek and Bierkens, 2008; Best et al., 2011). Early efforts focussed on the simulation of natural water resources and the impacts of land cover and climate change on water availability (Oki et al., 1995; Nijssen et al., 2001a; Nijssen et al., 2001b). Recently, a larger focus has been on incorporating anthropogenic impacts, such as water withdrawals and dam operations, into water resource assessments (Alcamo et al., 2003; Haddeland et al., 2006b; Biemans et al., 2011; Wada et al., 2011b; Hanasaki et al., 2018).

Global water withdrawals increased eight-fold over the last century and are projected to increase further (Shiklomanov, 2000; Wada et al., 2011a). Although water withdrawals are only a small fraction of the total global runoff (Oki and Kanae, 2006), water scarcity can be severe due to the variability of water in both time and space (Postel et al., 1996). Already severe water scarcity is experienced by two-thirds of the global population for at least part of the year (Mekonnen and Hoekstra, 2016). To stabilize water availability for different sectors (e.g. irrigation, hydropower, and domestic uses) dams and reservoirs were built, which are able to strongly affect global river streamflow (Nilsson et al., 2005; Grill et al., 2019). In addition, groundwater resources are being extensively exploited to meet increasing water demands (Rodell et al., 2009; Famiglietti, 2014).

One of widely-used macro-scale hydrological models is the Variable Infiltration Capacity (VIC) model. The model was originally developed as a land-surface model (Liang et al., 1994), but has been mostly used as a stand-alone hydrological model (Abdulla et al., 1996; Nijssen et al., 1997) using an offline routing module (Lohmann et al., 1996; Lohmann et al., 1998a, b). Where land-surface models focus on the vertical exchange of water and energy between the land surface and the atmosphere, hydrological models focus on the lateral movement and availability of water. By combining these two approaches, VIC simulations are strongly process-based and this, in turn, provides a good basis for climate-impact modelling.

VIC has been used extensively in studies ranging from: coupled regional climate model simulations (Zhu et al., 2009; Hamman et al., 2016), combined river streamflow and water-temperature simulations (van Vliet et al., 2016), hydrological sensitivity to climate change (Hamlet and Lettenmaier, 1999; Nijssen et al., 2001a; Chegwidden et al., 2019), global streamflow simulations (Nijssen et al., 2001b), sensitivity in flow regulation and redistribution (Voisin et al., 2018; Zhou et al., 2018), and real-time drought forecasting (Wood and Lettenmaier, 2006; Mo, 2008). Several studies used VIC to simulate the anthropogenic impacts of irrigation and dam operation on water resources (Haddeland et al., 2006a; Haddeland et al., 2006b; Zhou et al., 2015; Zhou et al., 2016) based on the model setup of Haddeland et al. (2006b). However, further developments were needed to holistically assess anthropogenic impacts on global water resources using VIC (Nazemi and Wheater, 2015a, b; Döll et al., 2016; Pokhrel et al., 2016).

Firstly, the VIC model did not yet include groundwater withdrawals or water withdrawals from domestic, manufacturing and energy (thermoelectric) sources. Although these sectors use less water than irrigation (Shiklomanov, 2000; Grobicki et al., 2005; Hejazi et al., 2014) they are locally important actors (Gleick et al., 2013), especially for the water-food-energy nexus (Bazilian et al., 2011). Sufficient water supply and availability are essential for meeting a range of local and global sustainable development goals related to water, food, energy and ecosystems (Bijl et al., 2018). Secondly, environmental flow requirements (EFRs) were often neglected (Pastor et al., 2014), even though they are "necessary to sustain aquatic ecosystems which, in turn, support human cultures, economies, sustainable livelihoods, and well-being" (Brisbane Declaration, 2017). Anthropogenic alterations already strongly affect freshwater ecosystems (Carpenter et al., 2011), with more than a quarter of all global rivers experiencing very high biodiversity threats (Vorosmarty et al., 2010). By neglecting EFRs, sustainable water availability for anthropogenic uses is overestimated (Gerten et al., 2013). Lastly, while the model setup of Haddeland et al. (2006b) already included important anthropogenic impact modules (i.e. irrigation and dam operation), these were not fully integrated yet. Therefore multiple successive model runs were required (see Section 2.1) which was computationally expensive, especially for global water resources assessments.

Recently version 5 of the VIC model (VIC-5) was released (Hamman et al., 2018), which focussed on improving the VIC model infrastructure. These improvements provide the opportunity to fully integrate human-impacts into the VIC model framework, while reducing computation times. Here the newly developed VIC-WUR model is presented (named after the developing team at Wageningen University and Research). The VIC-WUR model extends the existing VIC-5 model with several modules that simulate the anthropogenic impacts on water resources. These modules will implement previous major works on anthropogenic impact modelling as well as integrate environmental flow requirements into VIC-5. The modules include: (1) integrated routing, (2) surface and groundwater use for various sectors (irrigation, domestic, industrial, energy and livestock), (3) environmental flow requirements for both surface and groundwater systems, and (4) dam operation.

The next section first describes the original VIC-5 hydrological model (Section 2.1), which calculates natural water resource availability. Subsequently the integration of the anthropogenic impact modules, which modify the water resource availability, are described (Section 2.2). Global anthropogenic water uses for each sector are also estimated (Section 2.3). To assess the capability of the newly developed modules, the VIC-WUR results were compared with FAO national water withdrawals by sector and by source (FAO, 2016); Huang et al. (2018), Steinfeld et al. (2006), and Shiklomanov (2000) data on water withdrawals by sector; GRACE terrestrial water storage anomalies (NASA, 2002); GRDC streamflow timeseries (GRDC, 2003); and Yassin et al. (2019) and Hanasaki et al. (2006) data on reservoir operation (Section 3.2). VIC-WUR simulations results are also compared with various other state-of-the-art global hydrological models. Lastly, the impacts of adhering to surface and groundwater environmental flow requirements on water availability are assessed (Section 3.3). This assessment is included to indicate the effects of the newly integrated surface and groundwater environmental flow requirements on worldwide water availability.

2 Model development

2.1 VIC hydrological model

The basis of the VIC-WUR model is the Variable Infiltration Capacity model version 5 (VIC-5) (Liang et al., 1994; Hamman et al., 2018). VIC-5 is an open source macro-scale hydrological model that simulates the full water and energy balance on a (latitude – longitude) grid. Each grid cell accounts for sub-grid variability in land cover and topography, and allows for variable saturation across the grid cell. For each sub-grid the water and energy balance is computed individually (i.e. sub-grid do not exchange water or energy between one another). The methods used to calculate the water and energy balance are summarized in Appendix A, mainly based on the work of Liang et al. (1994). For the description of the global calibration and validation of the water balance one is referred to Nijssen et al. (2001b).

VIC version 5 (Hamman et al., 2018) upgrades did not change the model representation of physical processes, but improved the model infrastructure. Improvements include the use of NetCDF for input/output and the implementation of parallelization through Message Passing Interface (MPI). These changes increase computational speed and make VIC-5 better suited for (computationally expensive) global simulations. The most significant modification that enables new model applications is that VIC-5 also changed the processing order of the model. In previous versions all timesteps were processed for a single grid cell before continuing to the next cell (time-before-space). In VIC-5 all grid cells are processed before continuing to the next timestep (space-before-time). This development allows for interaction between grid cells every timestep, which is important for full integration of the anthropogenic impact modules, especially water withdrawals and dam operation.

For example, surface and subsurface runoff routing to produce river streamflow was typically done as a post-process operation (Lohmann et al., 1996; Hamman et al., 2017), due to the time-before-space processing order of previous versions. In order for reservoirs to account for downstream water demand, an irrigation demand initialization was required. This initialization could either be an independent offline dataset (Voisin et al., 2013a) or multiple successive model runs (Haddeland et al., 2006b). Since VIC-5 uses the space-before-time processing order, irrigation water demands and runoff routing could be simulated each timestep. The routing post-process was replaced by our newly developed routing module,

which simulates routing sequentially (upstream-to-downstream) based on the Lohmann et al. (1996) equations.

2.2 Anthropogenic-impact modules

VIC-WUR extends the existing VIC-5 though the addition of several newly implemented anthropogenic-impact modules (Figure 1). These modules include sector-specific water withdrawal and consumption, environmental flow requirements for both surface and groundwater systems and dam operation for large and small (within-grid) dams.

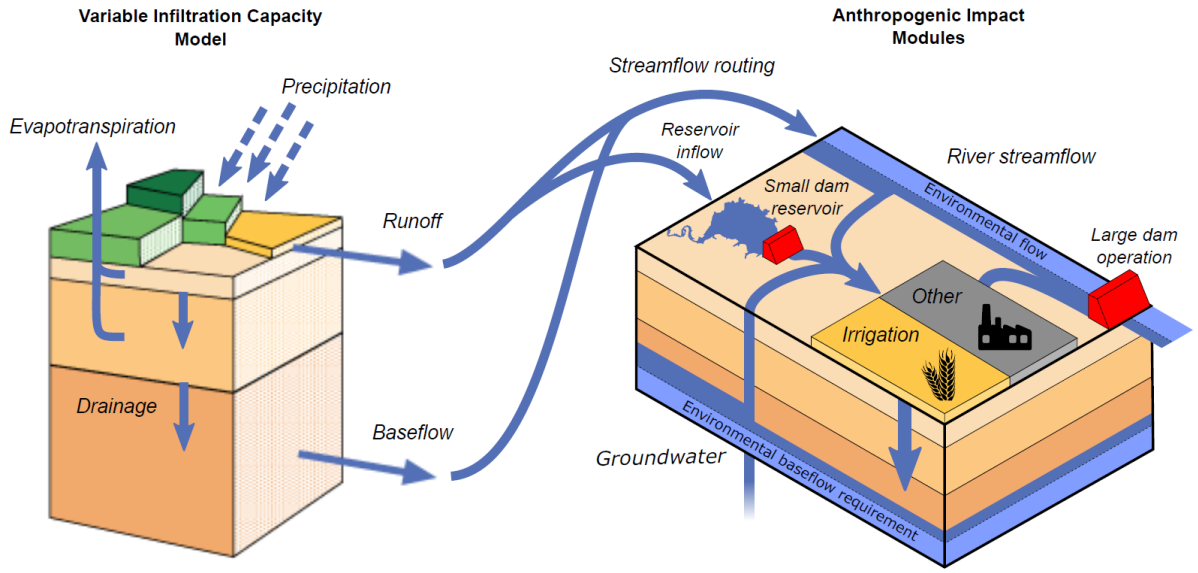

Figure 1: Schematic overview of the VIC-WUR model that includes the VIC-5 model and several anthropogenic impact modules. Water from river streamflow, groundwater and small (within-grid) reservoirs are available for withdrawal. Surface and groundwater withdrawals are constrained by environmental flow requirements. Withdrawn water is available for irrigation, domestic, industrial, energy and livestock use. Unconsumed irrigation water is returned to the soil column of the hydrological model. Unconsumed water for the other sectors is returned to the river streamflow. Small reservoirs fill using surface runoff from the cell they are located, while large dam reservoirs operate solely on rivers streamflow.

2.2.1 Water withdrawal and consumption

In VIC-WUR, sectoral water demands need to be specified for each grid cell (Section 2.3). To meet water demands, water can be withdrawn from river streamflow, small (within-grid) reservoirs, and groundwater resources. Streamflow withdrawals are abstracted from the grid cell discharge (as generated by the routing module) and reservoir withdrawals are abstracted from small dam reservoirs (located in the cell). Groundwater withdrawals are abstracted from the third layer soil moisture and an (unlimited) aquifer below the soil column. Aquifer abstractions represent renewable and non-renewable

158 abstractions from deep groundwater resources. Subsurface runoff is used to fill the aquifer if there is a
159 deficit.

160 The partitioning of water withdrawals between surface and ground water resources is data driven
161 (similar to e.g. Döll et al., 2012; Voisin et al., 2017; Hanasaki et al., 2018). Partitioning was based on
162 the study of Döll et al. (2012), who estimated groundwater withdrawal fractions for each sector in around
163 15.000 national and sub-national administrative units. These groundwater fractions were based mainly
164 on information from the International Groundwater Resources Assessment Centre (IGRAC; un-
165 igrac.org) database. Surface water withdrawals were partitioned between river streamflow and small
166 reservoirs relative to water availability. Groundwater withdrawals were first withdrawn from the third
167 soil layer, second from the (remaining) river streamflow resources and lastly from the groundwater
168 aquifer. This order was implemented to avoid overestimation of non-renewable groundwater
169 withdrawals as a result of errors in the partitioning data. Aquifer withdrawals are additionally limited
170 by the pumping capacity from Sutanudjaja et al. (2018), who estimated regional pumping capacities
171 based on information from IGRAC.

172 Water can also be withdrawn from the river streamflow of other 'remote' cells in delta areas. Since
173 rivers cannot split in the routing module, the model is unable to simulate the redistribution of water
174 resources in dendritic deltas. Therefore, streamflow at the river mouth is available for use in delta areas
175 (partitioned based on demand) to simulate the actual water availability. Delta areas were delineated by
176 the global delta map of Tessler et al. (2015).

177 In terms of water allocation, under conditions where water demands cannot be met, water withdrawals
178 are allocated to the domestic, energy, manufacturing, livestock and irrigation sector in that order.
179 Withdrawn water is partly consumed, meaning the water evaporates and does not return to the
180 hydrological model. Consumption rates were set at 0.15 for the domestic and 0.10 for the industrial
181 sector, based on the data of Shiklomanov (2000). The water consumption in the energy sector was based
182 on Goldstein and Smith (2002) and varies per thermoelectric plant based on the fuel type and cooling
183 system. For the livestock sector the assumption was made that all withdrawn water is consumed.
184 Unconsumed water withdrawals for these sectors are returned as river streamflow. For the irrigation

sector, consumption was determined by the calculated evapotranspiration. Unconsumed irrigation water remains in the soil column and eventually returns as subsurface runoff.

2.2.2 Environmental flow requirements

Water withdrawals can be constrained by environmental flow requirements (EFRs). These EFRs specify the timing and quantity of water needed to support terrestrial river ecosystems (Smakhtin et al., 2004; Pastor et al., 2019). Surface and groundwater withdrawals are constrained separately in VIC-WUR, based on the EFRs for streamflow and baseflow respectively. EFRs for streamflow specify the minimum river streamflow requirements while EFRs for baseflow specify the minimum subsurface runoff requirements (from groundwater to surface water). Since baseflow is a function groundwater availability, baseflow requirements are used to constrain groundwater (including aquifer) withdrawals.

Various EFR methods are available (Smakhtin et al., 2004; Richter et al., 2012; Pastor et al., 2014). Our study used the Variable Monthly Flow (VMF) method (Pastor et al., 2014) to calculate the EFRs for streamflows. VMF calculates the required streamflow as a fraction of the natural flow during high (30 %), intermediate (45 %) and low (60 %) flow periods, as described in Appendix B. The VMF method performed favourably compared to other hydrological methods, in 11 case studies where EFRs were calculated locally (Pastor et al., 2014). The advantage of the VMF method is that the method accounts for the natural flow variability, which is essential to support freshwater ecosystems (Poff et al., 2010).

EFR methods for baseflow have been rather underdeveloped compared to EFR methods for streamflow. However, a presumptive standard of 90 % of the natural subsurface runoff through time was proposed by Gleeson and Richter (2018), as described in Appendix B. This standard should provide high levels of ecological protection, especially for groundwater dependent ecosystems.

Note that part of the EFRs for baseflow are already captured in the EFRs for streamflow, especially during low-flow periods that are usually dominated by baseflows. However, the EFRs for baseflow specifically limit local groundwater withdrawals while EFRs for streamflow include the accumulated runoff from upstream areas. Also, the chemical composition of groundwater derived flows is inherently

different, making them a non-substitutable water flow for environmental purposes (Gleeson and Richter, 2018).

2.2.3 Dam operation

Due to the lack of globally available information on local dam operations, several generic dam operation schemes were developed for macro-scale hydrological models to reproduce the effect of dams on natural streamflow (Haddeland et al., 2006a; Hanasaki et al., 2006; Zhao et al., 2016; Rougé et al., 2019; Yassin et al., 2019). In VIC-WUR a distinction is made between 'small' dam reservoirs (with an upstream area smaller than the cell area) and 'large' dam reservoirs, similar to Hanasaki et al. (2018), Wisser et al. (2010a) and Döll et al. (2009). Small dam reservoirs act as buckets that fill using surface runoff of the grid-cell they are located in and reservoirs storage can be used for water withdrawals in the same cell. Large dam reservoirs are located in the main river and used the operation scheme of Hanasaki et al. (2006), as described in Appendix C.

The scheme distinguishes between two dam types: (1) dams that do not account for water demands downstream (e.g. hydropower dams or flood protection dams) and (2) dams that do account for water demand downstream (e.g. irrigation dams). For dams that do not account for demands, dam release is aimed at reducing annual fluctuations in discharge. For dams that do account for demands, dam release is additionally adjusted to provide more water during periods of high demand. The operation scheme was validated by Hanasaki et al. (2006) for 28 reservoirs and was used in various other studies (Hanasaki et al., 2008b; Döll et al., 2009; Pokhrel et al., 2012b; Voisin et al., 2013b; Hanasaki et al., 2018). Here, the scheme was adjusted slightly to account for monthly varying EFRs and to reduce overflow releases, which is described in Appendix C.

The Global Reservoir and Dam (GRanD) database (Lehner et al., 2011) was used to specify location, capacity, function (purpose), and construction year of each dam. The capacity of multiple (small- and large) dams located in the same cell were combined.

2.3 Sectoral water demands

VIC-WUR water withdrawals are based on the irrigation, domestic, industry, energy and livestock water demand in each grid-cell. Water demands represent the potential water withdrawal, which is reduced when insufficient water is available. Irrigation demands were estimated based on the hydrological model while water demands for other sectors are provided to the model as an input. Domestic and industrial were estimated based on several socioeconomic predictors, while energy and livestock water demands were derived from power plant and livestock distribution data. Due to data limitations the energy sector was incomplete, and energy water demands were partly included in the industrial water demands (which combined the remaining energy and manufacturing water demands). For more details concerning sectoral water demand calculations the reader is referred to Appendix D.

2.3.1 Irrigation demands

Irrigation demands were set to increase soil moisture in the root zone so that water availability is not limiting crop evapotranspiration and growth. The exception is paddy rice irrigation (Brouwer et al., 1989), where irrigation was also supplied to keep the upper soil layer saturated. Water demands for paddy irrigation practices are relatively high compared to conventional irrigation practices due to increased evaporation and percolation. Therefore, the crop irrigation demands for these two irrigation practices were calculated and applied separately (i.e. in different sub-grids). Note that multiple cropping seasons are included based on the MIRCA2000 land-use dataset (Portmann et al., 2010) (see Section 3.1 for more details).

Total irrigation demands also included transportation and application losses. Note that transportation and application losses are not ‘lost’ but rather returned to the soil column without being used by the crop. The water loss fraction was based on Frenken and Gillet (2012), who estimated the aggregated irrigation efficiency for 22 United Nations sub-regions. Irrigation efficiencies were estimated based on the difference between AQUASTAT reported irrigation water withdrawals and calculated irrigation water requirements (Allen et al., 1998), using data on crop information (e.g. growing season, harvest area) from AQUASTAT.

2.3.2 Domestic and industrial demands

Domestic and industrial water withdrawals were estimated based on Gross Domestic Product (GDP) per capita and Gross Value Added (GVA) by industries respectively (from Bolt et al. (2018), Feenstra et al. (2015) and World bank (2010); see Appendix D for more details). These drivers do not fully capture the multitude of socioeconomic factors that influence water demands (Babel et al., 2007). However, the wide availability of data allows for extrapolation of water demands to data-scarce regions and future scenarios (using studies such as Chateau et al. (2014)).

Domestic water demands per capita (used for drinking, sanitation, hygiene and amenity uses) were estimated similar to Alcamo et al. (2003). Demands increased non-linearly with GDP per capita due to the acquisition of water using appliances as household become richer. A minimum water supply is needed for survival, and the saturation of water using appliances sets a maximum on domestic water demands. Industrial water demands (used for cooling, transportation and manufacturing) were estimated similar to Flörke et al. (2013) and Voß and Flörke (2010). Industrial demands increased linearly with GVA (as an indicator of industrial production). Since industrial water intensities (i.e. the water use per production unit) vary widely between different industries (Flörke and Alcamo, 2004 ; Vassolo and Döll, 2005; Voß and Flörke, 2010), the average water intensity was estimated for each country. Both domestic and industrial water demands were also influenced by technological developments that increase water-use efficiency over time, as in Flörke et al. (2013).

Domestic water demands varied monthly based on air temperature variability as in Huang et al. (2018) (based on Wada et al. (2011b)). Using this approach, water demands were higher in summer than in winter, especially for counties with strong seasonal temperature differences. Domestic water demand per capita were downscaled using the HYDE3.2 gridded population maps (Goldewijk et al., 2017). Industrial water demands were kept constant throughout the year. Industrial demands were downscaled from national to grid cell values using the NASA Back Marble night-time light intensity map (Roman et al., 2018). National industrial water demands were allocated based on the relative light intensity per grid cell for each country.

2.3.3 Energy and livestock demands

Energy water demands (used for cooling of thermoelectric plants) were estimated using data from van Vliet et al. (2016). Water use intensity for generation (i.e. the water use per generation unit) was estimated based on the fuel and cooling system type (Goldstein and Smith, 2002), which was combined with the generation capacity. Note that the data only covered a selection of the total number of thermoelectric power plants worldwide. Around 27 % of the total (non-renewable) global installed capacity between 1980 and 2011 was included in the dataset due to lack of information on cooling system types for the majority of thermoelectric plants. To avoid double counting, energy water demands were subtracted from the industrial water demands.

Livestock water demands (used for drinking and animal servicing) were estimated by combining the Gridded Livestock of the World (GLW3) map (Gilbert et al., 2018) with the livestock water requirement reported by Steinfeld et al. (2006). Eight varieties of livestock were considered: cattle, buffaloes, horses, sheep, goats, pigs, chicken and ducks. Drinking water demands varied monthly based on temperature as described by Steinfeld et al. (2006), whereby drinking water requirements were higher during higher temperatures.

3 Model application

3.1 Setup

VIC-WUR results were generated between 1979 and 2016, excluding a spin-up period of one year (analysis period from 1980 to 2016). The model used a daily timestep (with a 6-hourly timestep for snow processes) and simulations were executed on a 0.5° by 0.5° grid (around 55 km at the equator) with three soil layers per grid cell. Soil and (natural) vegetation parameters were the same as in Nijssen et al. (2001c) (disaggregated to 0.5°), who used various sources to determine the soil (Cosby et al., 1984; Carter and Scholes, 1999) and vegetation parameters (Calder, 1993; Ducoudre et al., 1993; Sellers et al., 1994; Myneni et al., 1997).

Nijssen et al. (2001c) used the Advanced Very High Resolution Radiometer vegetation type database (Hansen et al., 2000) to spatially distinguish 13 land cover types. The land cover type ‘cropland’ in the

original land-cover dataset was replaced by cropland extents from the MIRCA2000 cropland dataset (Portmann et al., 2010). MIRCA2000 distinguishes the monthly growing area(s) and season(s) of 26 irrigated and rain-fed crop types around the year 2000. Crop types were aggregated into three land cover types: rain-fed, irrigated and paddy rice cropland. The natural vegetation was proportionally rescaled to make up discrepancies between the natural vegetation and cropland extents.

Cropland coverage (the cropland area actually growing crops) varied monthly based on the crop growing areas of MIRCA2000. The remainder was treated as bare soil. Cropland vegetation parameters (e.g. Leaf Area Index (LAI), displacement, vegetation roughness and albedo) vary monthly based on the crop growing seasons and the development-stage crop coefficients of the Food and Agricultural Organisation (Allen et al., 1998).

The latest WATCH forcing data Era Interim (aggregated to 6 hourly), developed by the EU Water and Global Change (WATCH; Harding et al., 2011) project, was used as climate forcing (WFDEI; Weedon et al., 2014). The dataset provides gridded historical climatic variables of minimum and maximum air temperature, precipitation (as the sum of snowfall and rainfall, GPCC bias-corrected), relative humidity, pressure and incoming shortwave and longwave radiation.

For naturalized simulations only the routing module was used. For the human-impact simulations the sectoral water withdrawals and dam operation modules were turned on in the model simulations. For the EFR-limited simulations water withdrawals and dam operations were constrained as described.

3.2 Validation and evaluation

In order to validate the VIC-WUR human-impact modules, water withdrawal, terrestrial total water storage anomalies, streamflow and reservoir operation simulations were compared with observations. The validation specifically focused on the effects of the newly included human-impact modules, meaning that streamflow and total-water storage anomaly results are shown for river basins that are strongly influenced by human activities. A general validation for streamflow and terrestrial total water storage anomalies (including basins with limited human activities) is shown in Appendix E.

3.2.1 Sectoral water withdrawals

Simulated global domestic, industrial, livestock and irrigation mean water withdrawals were 310, 771, 36 and 2202 km^3 $year^{-1}$ respectively for the period of 1980 to 2016. Sectoral water withdrawals were compared with FAO national annual water withdrawals (FAO, 2016), monthly withdrawal data from Huang et al. (2018) and annual withdrawal data from Shiklomanov (2000) and Steinfeld et al. (2006). For the latter studies, water withdrawals were aggregated by region (world, Africa, Asia, Americas, Europe and Oceania). Note that Huang et al. (2018) irrigation water withdrawals integrate results of four other macro-scale hydrological models (WaterGAP, H08, LPJmL, PCR-GLOBWB), using the same land-use and climate setup as our study. Results from individual macro-scale hydrological models are also shown.

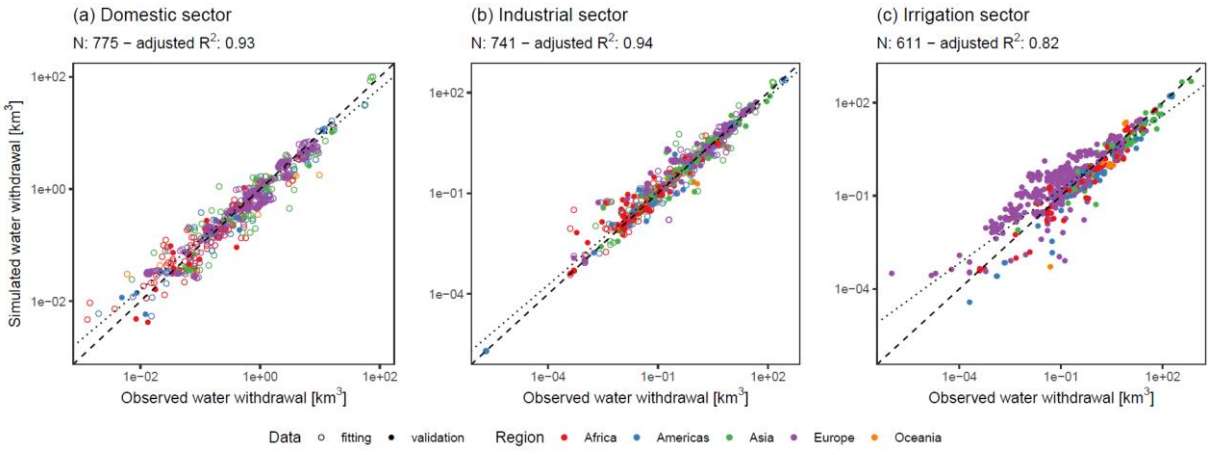

Figure 2: Comparison between simulated and reported national annual water withdrawals for the (a) domestic, (b) industrial and (c) irrigation sector. Colours distinguish between regions. Open circles were also used in the calibration of the water withdrawal demands. The dashed line indicates the 1:1 ratio and the spotted line indicates the simulated best linear fit. Note the log-log axis which is used to display the wide range of water withdrawals. The R^2 adjusted is also based on the log values.

Simulated domestic, industrial and irrigation water withdrawals correlated well to reported national water withdrawals, with adjusted R^2 of 0.93, 0.94 and 0.82 for domestic, industrial and irrigation water withdrawal respectively (Figure 2a-c). Generally, smaller water withdrawals were overestimated and larger water withdrawals were underestimated. Differences for the domestic and industrial sector were small and probably related to the fact that smaller countries were poorly delineated on a 0.5° by 0.5° grid. However, irrigation differences were larger with overestimations of irrigation water withdrawals in (mostly) Europe. Since irrigation water demands are the results of the simulated water balance,

overestimations would indicate a regional underestimation of water availability for Europe or differences in irrigation efficiency.

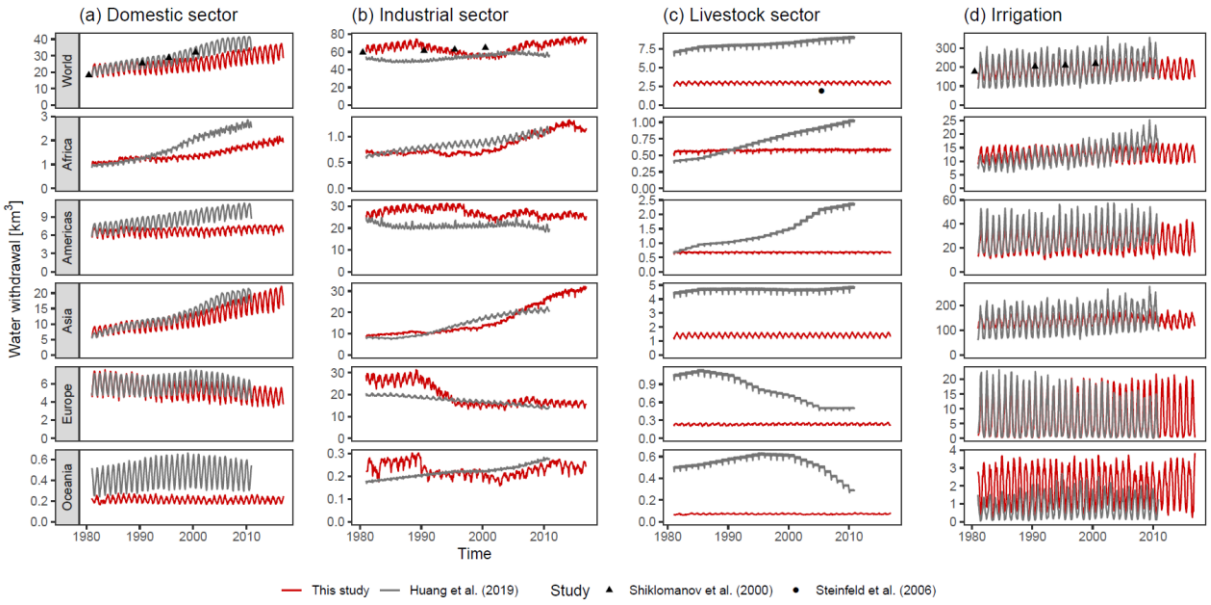

Figure 3: Comparison between simulated and compiled monthly and annual regional water withdrawals for the (a) domestic sector, (b) industrial sector, (c) livestock sector, and (d) irrigation. Colours and shapes distinguish between studies. Note that the jitter in livestock withdrawals is due to the different days per month.

When domestic, industrial and livestock water withdrawals were compared to other studies, results were mixed (figure 3a-c). Simulated domestic withdrawals followed a similar trend in time. However, simulated domestic water withdrawals trends were overall somewhat underestimated with a mean bias of 54 km^3 $year^{-1}$ compared to Huang et al. (2018). Asia is the main contributor to the global underestimation, but results are similar in most regions. Simulated industrial water withdrawal were (mostly) higher in our study with a mean bias of 107 km^3 $year^{-1}$ compared to Huang et al. (2018) but only a mean bias of 5 km^3 $year^{-1}$ compared to Shiklomanov (2000). Also, industrial water withdrawal trends in time were less consistent.

Withdrawal differences for the domestic and industrial sector are probably due to the limited data availability. Our approach to compute water demands was data-driven and sensitive to data gaps (as opposed to Huang et al. (2018) who also combined model results). For example, domestic withdrawal data for China was not available before 2007 and industrial withdrawal data was limited before 1990. Also, data on the disaggregation of industrial sectors (e.g. energy and mining) was limited, which can be important sectors in the water-food-energy nexus.

For livestock water withdrawals there is a large discrepancy between the Huang et al. (2018) and Steinfeld et al. (2006). Both studies used similar livestock maps, but there was large differences in livestock water intensity [litre animal^{-1} year^{-1}]. Since our study used Steinfeld et al. (2006) to estimate livestock water intensity, our results were closer to their values (slightly higher due to the inclusion of buffaloes, horses and ducks). Note that Huang et al. (2018) shows trends in livestock water withdrawals while our study used static livestock maps.

Table 1: Global irrigation water withdrawals as calculated by several global hydrological models. **Includes livestock withdrawals.

Model	Irrigation withdrawal [km^3 year^{-1}]	Representative years	Reference
VIC-WUR	2202 (± 60)	1980-2016	Our study
H08	(a) 2810 (b) 2544 (± 75)	(a) 1995 (b) 1984 - 2013	(a) Hanasaki et al. (2008a) (b) Hanasaki et al. (2018)
MATSIRO	(a) 2158 (± 134) (b) 3028 (± 171)	(a) 1983 - 2007 (b) 1998 - 2002	(a) Pokhrel et al. (2012a) (b) Pokhrel et al. (2015)
LPJmL	2555	1971 - 2000	Rost et al. (2008)
PCR-GLOB	(a) 2644 (b) 2309 **	(a) 2010 (b) 2000 - 2015	(a) Wada and Bierkens (2014) (b) Sutanudjaja et al. (2018)
WaterGAP	(a) 3185 (b) 2400	(a) 1998-2002 (b) 2003 - 2009	(a) Döll et al. (2012) (b) Döll et al. (2014)
WBM	2997	2002	Wisser et al. (2010b)

Simulated irrigation water withdrawals were within range of other macro-scale hydrological model estimates (Table 1). Simulated monthly variability in irrigation water withdrawals is reduced compared to the compiled results of Huang et al. (2018) (Figure 3d), especially in Asia. Also, trends in time are less pronounces as can be seen in Africa. These differences may indicate a relative low weather/climate sensitivity of evapotranspiration in VIC-WUR, as annual and interannual weather changes affect irrigation water demands to a lesser degree.

3.2.2 Groundwater withdrawals and depletion

Simulated global mean withdrawals were 2327 and 992 km^3 year^{-1} for surface and groundwater respectively for the period of 1980 to 2016. Of the global groundwater withdrawals, 334 km^3 year^{-1}

contributed to groundwater depletion. Simulated ground and surface water withdrawals and terrestrial total water storage anomalies were compared FAO national annual water withdrawals (FAO, 2016) and monthly storage anomaly data from the GRACE satellite (NASA, 2002). GRACE satellite total water storage anomalies were used to validate total water storage dynamics as well as groundwater exploitation contributing to downward trends in total water storage. Groundwater depletion results from other macro-scale hydrological models are shown as well. In order to compare the simulation results to the GRACE dataset, a 300km gaussian filer was applied to the simulated data (similar to Long et al. (2015)).

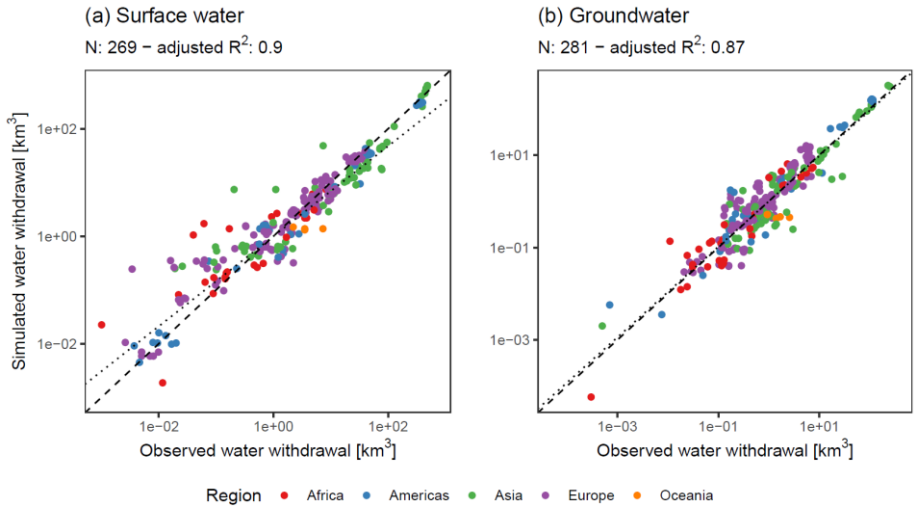

Figure 4: Comparison between simulated and reported national annual water withdrawals from (a) surface water and (b) groundwater. Colours distinguish between regions. The dashed line indicates the 1:1 ratio and the spotted line indicates the simulated best linear fit. Note the log-log axis which is used to display the wide range of water withdrawals. The R^2 adjusted is also based on the log values.

Simulated surface and groundwater withdrawals correlated well to the reported national water withdrawals, with adjusted R^2 of 0.90 and 0.87 for surface and groundwater respectively (Figure 4a-b). Surface water withdrawals were overestimated for low withdrawals and underestimated for large withdrawals. There is a weak correlation (-0.35) between the underestimations in surface water withdrawals and the overestimation in groundwater withdrawals, meaning water withdrawal differences could be related to the partitioning between surface and groundwater resources. Also, it is likely that low water demands are overestimated (as discussed in Section 3.2.1), resulting in an overestimation of low surface water withdrawals.

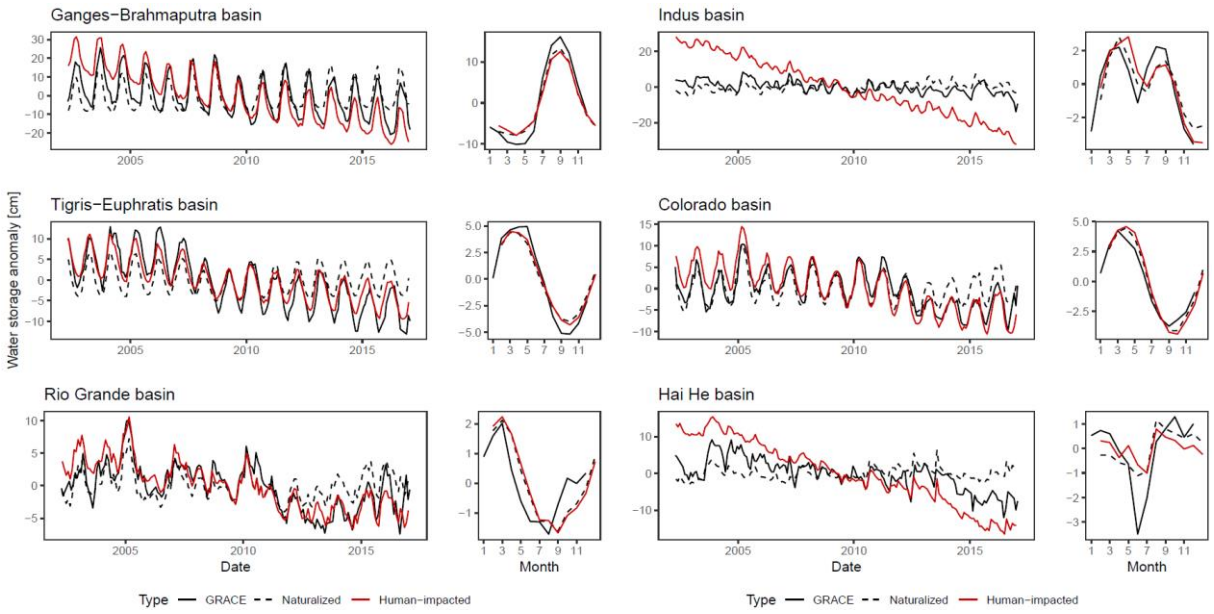

Figure 5: Comparison between simulated and observed monthly terrestrial total water storage anomalies. Figures indicate timeseries and multi-year mean average for naturalized simulations (dashed), human-impacted simulations (red) and observed (black) terrestrial total water storage anomalies.

Simulated monthly terrestrial water storage anomalies correlated well to the GRACE observations, with mean annual and inter-annual Root Mean Squared Error (RMSE) of 1.9 mm and 3.5 mm respectively. The difference between annual and inter annual performance was primarily due to the groundwater depletion process (Figure 5). Simulated groundwater depletion was (mostly) overestimated (e.g. Indus and Hai He basins), with higher declining trends in terrestrial total water storage for most basins. However, compared to other macro-scale hydrological models, simulated groundwater withdrawal and exploitation was within range (Table 2), even though total groundwater withdrawals were relatively high.

As with the FAO comparison, these results seems to indicate that withdrawal partitioning towards groundwater is overestimated. However, conclusions regarding groundwater depletion are limited by the relatively simplistic approach to groundwater used in our study (as discussed by Konikow (2011) and de Graaf et al. (2017)). For example, processes such as wetland recharge and groundwater flows between cells are not simulated, even though these could decrease groundwater depletion.

Table 2: Global groundwater withdrawals and depletion as calculated by several global hydrological models.

Model	Groundwater withdrawal [km3 year-1]	Groundwater depletion [km3 year-1]	Representative years	Reference

VIC-WUR	992 (± 51)	316 (± 63)	1980 - 2016	Our study
H08	789 (± 30)	182 (± 26)	1984 - 2013	Hanasaki et al. (2018)
MATSIRO	570 (± 61)	330	1998 - 2002	Pokhrel et al. (2015)
GCAM		(a) 600 (b) 550	(a) 2005 (b) 2000	(a) Kim et al. (2016) (b) Turner et al. (2019)
PCR-GLOB	(a) 952 (b) 632	(a) 304 (b) 171	(a) 2010 (b) 2000 - 2015	(a) Wada and Bierkens (2014) (b) Sutanudjaja et al. (2018)
WaterGAP	(a) 1519 (b) 888	(a) 250 (b) 113	(a) 1998-2002 (b) 2000 - 2009	(a) Döll et al. (2012) (b) Döll et al. (2014)

3.2.3 Discharge modification

Simulated discharge was compared to GRDC station data (GRDC, 2003) for various human-impacted rivers. Stations were selected if the upstream area was larger than 20,000 km2, matched the simulated upstream area at the station location, and the available data spanned more than 2 years. Subsequently, stations where the human-impact modules did not sufficiently impacted discharge were omitted. In order validate the reservoir operation more thoroughly, simulated reservoir inflow, storage and release was compared with operation data from Hanasaki et al. (2006) and Yassin et al. (2019). Reservoirs were included if the simulated storage capacity (which is the combined storage capacity of all large dams in a grid) was similar to observed storage capacity.

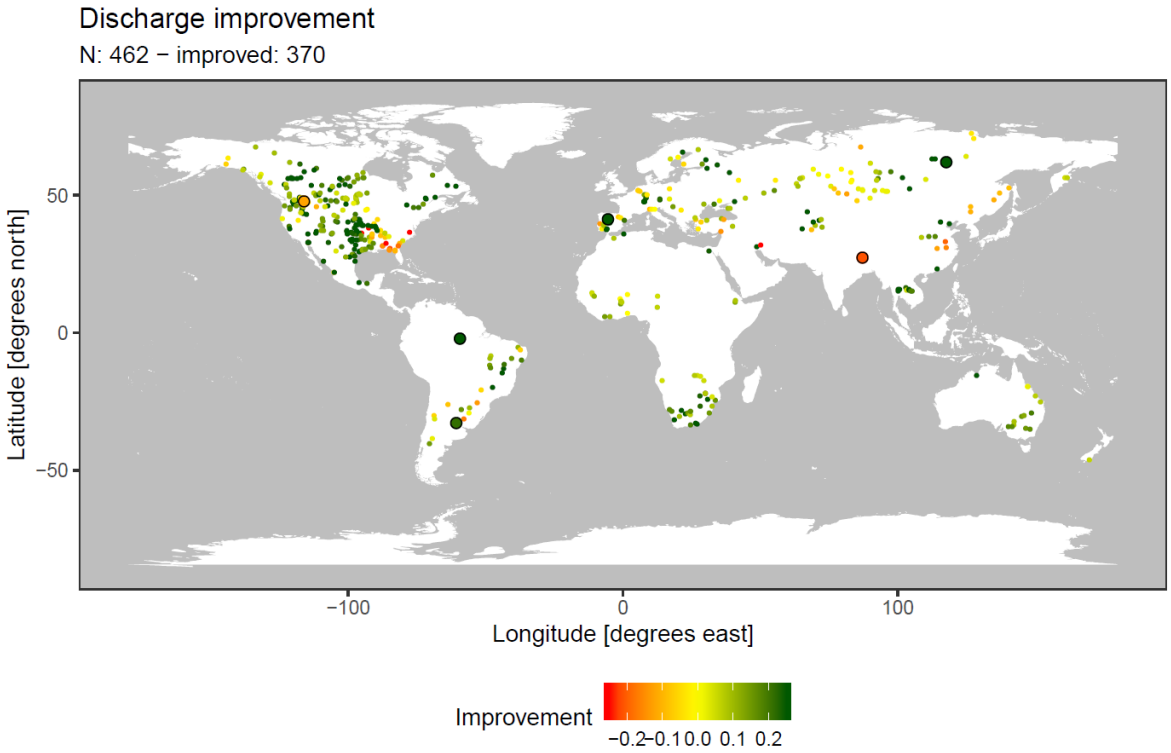

Figure 6: Discharge improvement from naturalized to human-impacted simulations (as a fraction of the naturalized RMSE). Circled larger stations are shown in Figure 7.

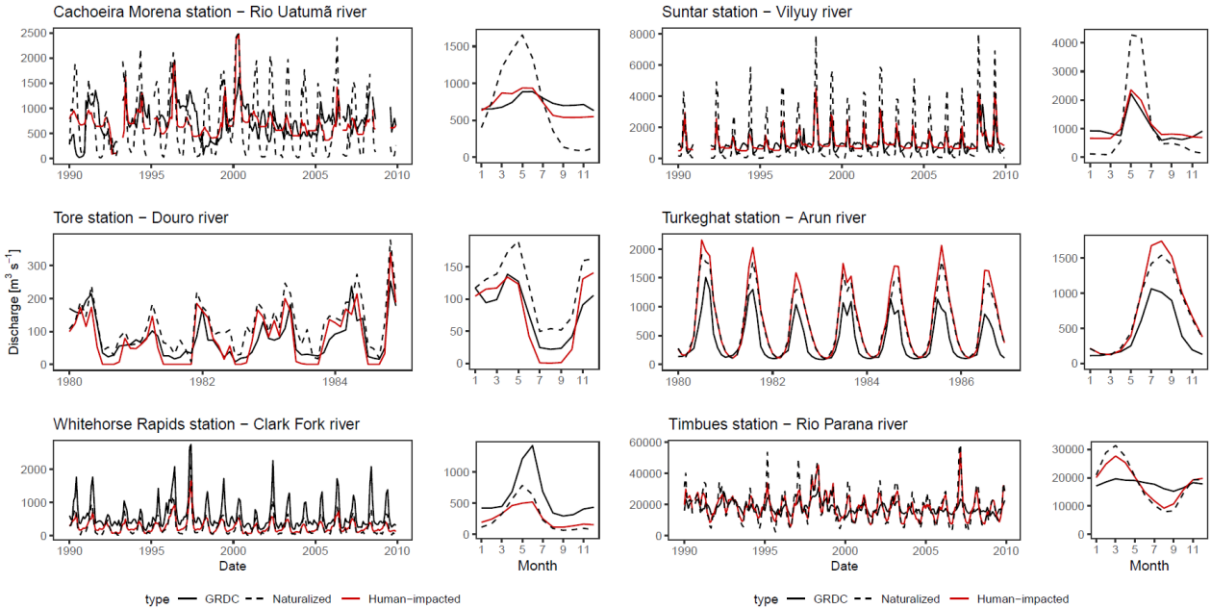

Figure 7: Comparison between simulated and observed discharge. Figures indicate timeseries and multi-year average of for naturalized simulations (dashed), human-impacted simulations (red) and observed (black) discharge.

The inclusion of the human-impact modules improved discharge performance, measured in RMSE, for 370 out of 462 stations (80 %; Figure 6 and 7). Improvements were mainly due to the effects of reservoir operation on discharges (e.g. Cachoeira Morena and Suntar stations), but also due to withdrawal

reductions (e.g. Tore station). Reservoir effects on discharge were sometimes underestimated however (e.g. Timbues station).

Decreased performance was mostly related to under or overestimations of (calibrated) natural streamflow which was subsequently exacerbated by reservoir operation and water withdrawals. For example, the Clark Fork river naturalized streamflow was underestimated, which was subsequently further underestimated by the human-impact modules (Whitehorse Rapids station). Also, increases in discharge due to groundwater withdrawals could increase naturalized streamflow (e.g. Turkeghat station). Further improvements to discharge performance would most likely require either a recalibration of the VIC model parameters.

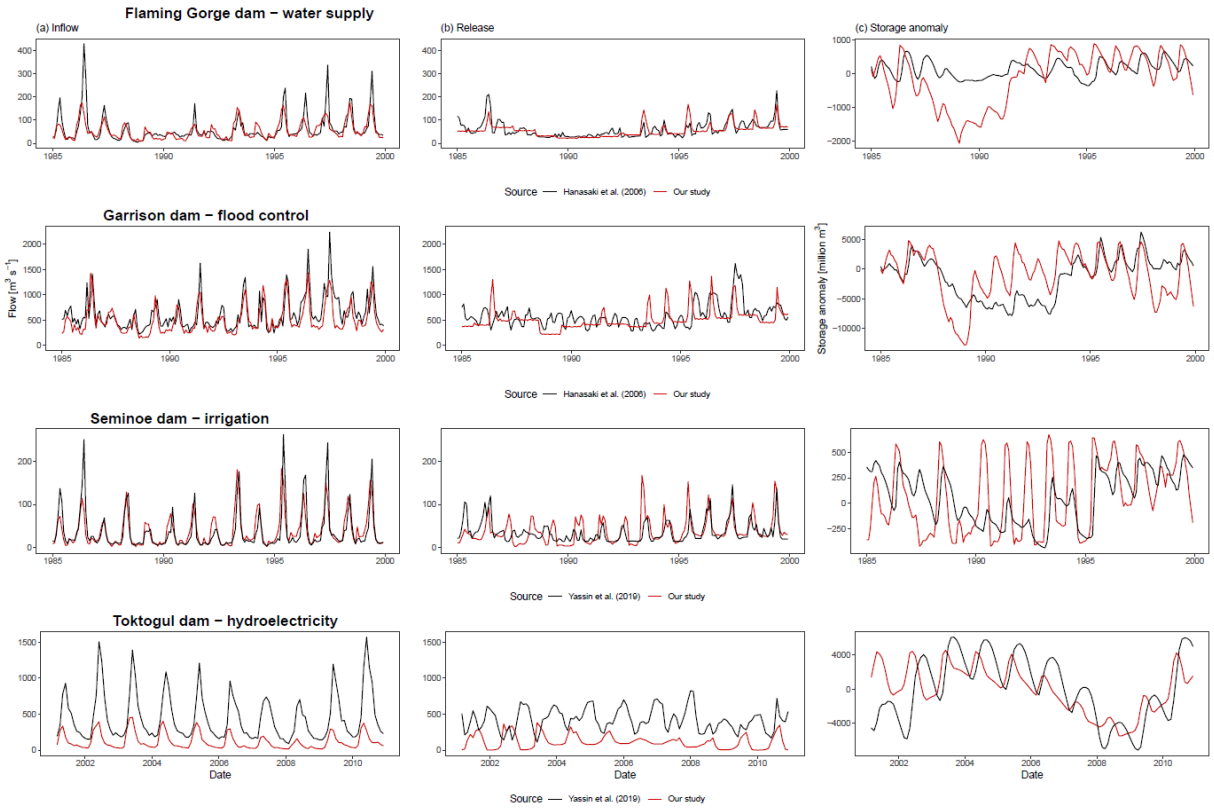

Figure 8: Comparison between simulated and observed reservoir operation. Figures indicate timeseries and multi-year averages of (a) inflow, (b) release and (c) storage anomalies for human-impacted simulations (red) and observations (black).

For individual reservoirs, operation characteristics were generally well simulated (Figure 8), with reductions in annual discharge variations (e.g. Flaming Gorge and Garrison dams) and increased water release for irrigation (e.g. Seminoe dam). However, due to changes in locally simulated and actual inflow, dam operation can take on different characteristics (e.g. Toktogul dam). Also, peak discharge

events caused by reservoir overflow (as also described by Masaki et al. (2018)) were not always sufficiently represented in the observations (e.g. Garisson dam). These differences indicate locally varying reservoir operation strategies. Several studies have developed reservoir operation schemes that can be calibrated to the local situation (Rougé et al., 2019; Yassin et al., 2019). However, worldwide implementations of these operation schemes remains limited by data availability.

3.3 Integrated environmental flow requirements

In order to assess the impact and capabilities of the newly integrated environmental flow requirements (EFRs) module, simulated water withdrawals with and without adhering to EFRs were compared.

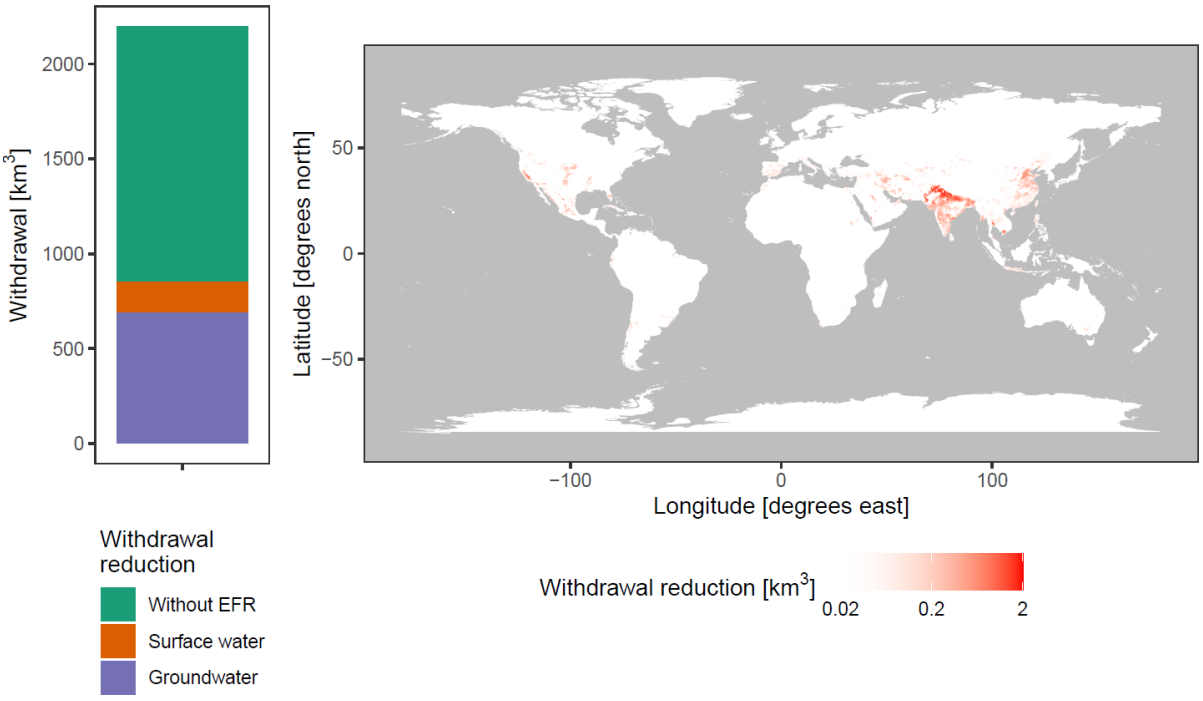

Figure 9: Average annual irrigation water withdrawal reductions when adhering to EFRs as (left) global gross total and (right) spatially distributed. Global gross totals are separated into withdrawals without any reduction (green), surface water withdrawal reductions (orange) and groundwater withdrawal reductions (purple). Note the log axis for the spatially distributed withdrawal reductions to better display the spatial distribution of the reductions.

If water-use would be limited to EFRs, irrigation withdrawals would need to be reduced by about 39 % (851 km^3 $year^{-1}$) (Figure 9a). Under the strict requirements used in our study, 81 % (693 km^3 $year^{-1}$) of the reduction could be attributed to limitations imposed on groundwater withdrawals. Subsequently, the impact of the environmental flow requirements (if adhered to) would be largest in groundwater dependent regions (Figure 9b). Note that, due to the full integration of EFRs, downstream surface water

withdrawals increased by 98 km^3 $year^{-1}$ when limiting groundwater withdrawals on top of limiting surface water withdrawals, due to increase subsurface runoff.

Reductions due to EFRs were similar to Jägermeyr et al. (2017), who calculated irrigation withdrawal reductions of 41 % (997 km^3 $year^{-1}$) assuming only surface water abstractions. In our study, surface water reductions were smaller since the strict groundwater requirements increases subsurface runoff to surface waters. It can be discussed to what extent the EFRs for baseflow were too constricting, since they were based on the relatively stringent EFR for streamflow of Richter et al. (2012) (10 % of the natural streamflow). However, in the absence of any other standards, this baseflow standard remains the best available. Note that, even when accounting for EFRs for baseflow on a grid scale, withdrawals could still have local and long-term impacts that are not captured by the model. The timing, location and depth of groundwater withdrawals are important factors due to their interactions with the local geohydrology, as discussed by Gleeson and Richter (2018).

4 Conclusion

The VIC-WUR model introduced in this paper aims to provide new opportunities for global water resource assessments using the VIC model. Accordingly, several anthropogenic impact modules, based on previous major works, were integrated into the VIC-5 macro-scale hydrological model: domestic, industrial, energy, livestock and irrigation water withdrawals from both surface water and groundwater as well as an integrated environmental flow requirement module and dam operation module. Global gridded datasets on domestic, industrial, energy and livestock demand were developed separately and used to force the VIC-WUR model.

Simulated national water withdrawals were in line with reported national annual withdrawals (R^2 adjusted > 0.8; both per sector as per source). However, the data-oriented methodology used to derive sectoral water demands resulted in different withdrawal trends over time compared to other studies (Shiklomanov, 2000; Huang et al., 2018). While the current setup to estimate sectoral water demands is well suited for future water withdrawal estimations, there are various other approaches (e.g. Alcamo et al., 2003; Vassolo and Döll, 2005; Shen et al., 2008; Hanasaki et al., 2013; Wada and Bierkens, 2014).

As the model setup of VIC-WUR allows for the evaluation of other sectoral water demand inputs (on various temporal aggregations), several different approaches can be used depending on the focus region and data-availability for calibration. Terrestrial water storage anomaly trends were well simulated (mean annual and inter-annual RMSE of 1.9 mm and 3.6 mm respectively), while groundwater exploitation was overestimated. Overestimated groundwater depletion rates are likely related to an over-partitioning of water withdrawals to groundwater. The implemented human impact modules increased simulated discharge performance (370 out of 462 stations), mostly due to the effects of reservoir operation.

An assessment of the effect of EFRs shows that, when one would adhere to these requirements, global water withdrawals would be severely limited (39 %). This limitation is especially the case for groundwater withdrawals, which, under the strict requirements used in our study, need to be reduced by 81 %.

VIC-WUR has potential for studying impacts of climate change and anthropogenic developments on current and future water resources and sectoral specific-water scarcity. The additions presented here make the VIC model more suited for fully-integrated worldwide water-resource assessments and substantially decrease computation times compared to Haddeland et al. (2006a).

5 Code availability

All code for the VIC-WUR model is freely available at github.com/wur-wsg/VIC (tag VIC-WUR.2.1.0; DOI 10.5281/zenodo.3934325) under the GNU General Public License, version 2 (GPL-2.0). VIC-WUR documentation can be found at vicwur.readthedocs.io. The original VIC model is freely available at github.com/UW-Hydro/VIC (tag VIC.5.0.1; DOI 10.5281/zenodo.267178) under the GNU General Public License, version 2 (GPL-2.0). VIC documentation can be found at vic.readthedocs.io. Documentation and scripts concerning input data used in our study is freely available at github.com/bramdr/VIC_support (tag VIC-WUR.2.1.0; DOI 10.5281/zenodo.3934363) under the GNU General Public License, version 3 (GPL-3.0).

6 Appendix

6.1 Appendix A: VIC water and energy balance

In VIC each sub-grid computes the water and energy balance individually (i.e. sub-grid do not exchange water or energy between one another). For the water balance, incoming precipitation is partitioned between evapotranspiration, surface and subsurface runoff, and soil water storage. Potential evapotranspiration is based on the Penman-Monteith equation without the canopy resistance (Shuttleworth, 1993). The actual evapotranspiration is calculated by two methods, based on whether the land cover is vegetated or not (bare soil). Evapotranspiration of vegetation is constrained by stomatal, architectural and aerodynamic resistances and is partitioned between canopy evaporation and transpiration based on the intercepted water content of the canopy (Deardorff, 1978; Ducoudre et al., 1993). Bare soil evaporation is constrained by the saturated area of the upper soil layer. The saturated area is variable within the grid since (as the model name implies) the infiltration capacity of the soil is assumed heterogeneous (Franchini and Pacciani, 1991). Saturated areas evaporate at the potential evaporation rate while in unsaturated areas evaporation is limited. Surface runoff is produced by precipitation over saturated areas. Precipitation over unsaturated areas infiltrates into the upper soil layer and drains through the soil layers based on the gravitational hydraulic conductivity equations of Brooks and Corey (1964). In the first and second layer water is available for transpiration, while the third layer is assumed to be below the root zone. From the third layer baseflow is generated based on the non-linear Arno conceptualization (Franchini and Pacciani, 1991). Baseflow increases linearly with soil moisture content when the moisture content is low. At higher soil moisture contents the relation is non-linear, representing subsurface storm-flows.

For the energy balance, incoming net radiation is partitioned between sensible, latent, and ground heat fluxes and energy storage in the air below the canopy. The energy storage below the canopy is omitted if it is considered negligible (e.g. the canopy surface is open or close to the ground). The latent heat flux is determined by the evapotranspiration as calculated in the water balance. The sensible heat flux is calculated based on the difference between the air and surface temperature and the ground heat flux is calculated based on the difference between the soil and surface temperature. Since the incoming net

radiation is also a function of the surface temperature (specifically the outgoing longwave radiation), the surface temperature is solved iteratively. Subsurface ground heat fluxes are calculated assuming an exponential temperature profile between the surface and the bottom of the soil column, where the bottom temperature is assumed constant. Later model developments included options for finite difference solutions of the ground temperature profile (Cherkauer and Lettenmaier, 1999), spatial distribution of soil temperatures (Cherkauer and Lettenmaier, 2003), a quasi-2-layer snow-pack snow model (Andreadis et al., 2009), and blowing snow sublimation (Bowling et al., 2004).

6.2 Appendix B: EFRs for surface and groundwater

VIC-WUR used the Variable Monthly Flow (VMF) method (Pastor et al., 2014) to limit surface water withdrawals. The VMF method (Pastor et al., 2014) calculates the EFRs for streamflow as a fraction of the natural flow during high (Eq. A.1), intermediate (Eq. A.2) and low (Eq. A.3) flow periods. The presumptive standard Gleeson and Richter (2018) is used to limit groundwater withdrawals (including aquifer groundwater withdrawals). This standard calculates the EFRs for baseflow as 90 % of the natural subsurface runoff through time (Eq. A.4). Here, daily instead of monthly EFRs were used to better capture the monthly flow variability.

$$EFR_{s,d} = 0.6 \cdot NF_{s,d} \quad \text{Eq. (A.1)}$$

$$where\ NF_{s,d} \leq 0.4 \cdot NF_{s,y}$$

$$EFR_{s,d} = 0.45 \cdot NF_{s,d} \quad \text{Eq. (A.2)}$$

$$where\ 0.4 \cdot MF_{s,y} < NF_{s,d} \leq 0.8 \cdot NF_{s,y}$$

$$EFR_{s,d} = 0.3 \cdot NF_{s,d} \quad \text{Eq. (A.3)}$$

$$where\ NF_{s,d} > 0.8 \cdot NF_{s,y}$$

$$EFR_{b,d} = 0.9 \cdot NF_{b,d} \quad \text{Eq. (A.4)}$$

Where $EFR_{s,d}$ is the daily EFRs for streamflow [$m^3\ s^{-1}$], $EFR_{b,d}$ the daily EFRs for baseflow [$m^3\ s^{-1}$], $NF_{s,d}$ is the average natural daily streamflow [$m^3\ s^{-1}$], and $NF_{s,y}$ is the average natural yearly streamflow [$m^3\ s^{-1}$], and $NF_{b,d}$ is the average natural daily baseflow [$m^3\ s^{-1}$].

EFRs for streamflow and baseflow were based on VIC-WUR naturalized simulations between 1980 and 2010. Average natural daily flows were calculated as the interpolated multi-year monthly average flow over the simulation period.

6.3 Appendix C: Dam operation scheme

VIC-WUR used a dam operation scheme based on Hanasaki et al. (2006). Target release (i.e. the estimated optimal release) was calculated at the start of the operational year. The operational year starts at the month where the inflow drops below the average annual inflow, and thus the storage should be at its desired maximum. The scheme distinguished between two dam types: (1) dams that did not account for water demands downstream (e.g. hydropower dams or flood control) and (2) dams that did account for water demands downstream (e.g. irrigation dams). The original scheme of Hanasaki et al. (2006) also accounts for EFRs, which were fixed at half the annual mean inflow. Other studies lowered the requirements to a tenth of the mean annual inflow, increasing irrigation availability and preventing excessive releases (Biemans et al., 2011; Voisin et al., 2013b). In our study the original dam operation scheme was adapted slightly to account for monthly varying EFRs.

For dams that did not account for demands, the initial release was set at the mean annual inflow corrected by the variable EFRs (Eq. A.5). For dams that did account for demands, the initial release was increased during periods of higher water demand. If demands were relatively high compared to the annual inflow, the release was corrected by the demand relative to the mean demand (Eq. A.6). If demands were relatively low compared to the annual inflow, release was corrected based on the actual water demand (Eq. A.7).

$$R'_m = EFR_{s,m} + (I_y - EFR_{s,y}) \quad \text{Eq. (A.5)}$$

$$where\ D_y = 0$$

$$R'_m = EFR_{s,m} + \left(I_y - EFR_{s,y}\right) * \frac{D_m}{D_y} \quad \text{Eq. (A.6)}$$

$$where\ D_y > 0\ and\ D_y > (I_y - EFR_{s,y})$$

$$R'_m = EFR_{s,m} + (I_y - EFR_{s,y}) - D_y + D_m \quad \text{Eq. (A.7)}$$

$$where\ D_y > 0\ and\ D_y \leq (I_y - EFR_{s,y})$$

Where R'_m is the initial monthly target release [$m^3\ s^{-1}$], $EFR_{s,m}$ is the average monthly EFR for streamflow demand [$m^3\ s^{-1}$], I_y is the average yearly inflow [$m^3\ s^{-1}$], $EFR_{s,y}$ is the average yearly EFR for streamflow [$m^3\ s^{-1}$], D_m is the average monthly water demand [$m^3\ s^{-1}$] and D_y is the average yearly water demand [$m^3\ s^{-1}$].

As in Hanasaki et al. (2006), the initial target release was adjusted based on storage and capacity. Target release was adjusted to compensate differences between the current storage and the desired maximum storage (Eq. A.8). Target release was additionally adjusted if the storage capacity is relatively low compared to the annual inflow, and unable to store large portions of the inflow for later release (Eq. A.9).

$$R_m = k \cdot R'_m \quad \text{Eq. (A.8)}$$

$$where\ c \geq 0.5$$

$$R_m = \left(\frac{c}{0.5}\right)^2 \cdot k \cdot R'_m + \left\{1 - \left(\frac{c}{0.5}\right)^2\right\} \cdot I_m \quad \text{Eq. (A.9)}$$

$$where\ 0 \leq c \leq 0.5$$

Where I_y is the average monthly inflow [$m^3\ s^{-1}$], c the capacity parameter [-] calculated as the storage capacity divided by the mean annual inflow and k the storage parameter [-] calculated as current storage divided by the desired maximum storage. The desired maximum storage was set at 85 % of the storage capacity as recommended by Hanasaki et al. (2006).

Water inflow, demand and EFRs were estimated based on the average of the past five years. Water demands were based on the water demands of downstream cells. Only a fraction of water demands were taken into account, based on the fraction of discharge the dam controlled. For example: if a dam controlled 70 % of the discharge of a downstream cell, than 70 % of its demands were taken into account. Fractions smaller than 25 % were ignored.

The original dam operation scheme of Hanasaki et al. (2006) was shown to produce excessively high discharge events due to overflow releases (Masaki et al., 2018). These overflow releases occurred due to a mismatch between the expected and actual inflow. In our study, dam release was increased during high-storage events to prevent overflow and accompanying high discharge events. If dam storage was above the desired maximum storage, target dam release was increased to negate the difference (Eq. A.10). If dam storage was below the desired minimum storage, release is decreased (Eq. A.11). Dam release was adjusted exponentially based on the relative storage difference: small storage differences were only corrected slightly, but if the dam was close to overflowing or emptying, the difference was corrected strongly.

$$R_a = R_m + \frac{(S - C\alpha)}{\gamma} \cdot \left(\frac{\frac{S}{C} - \alpha}{1 - \alpha} \right)^b \quad \text{Eq. (A.10)}$$

$$where\ S > C\alpha$$

$$R_a = R_m + \frac{(S - C(1-\alpha))}{\gamma} \cdot \left(\frac{(1-\alpha) - \frac{S}{C}}{1 - \alpha} \right)^b \quad \text{Eq. (A.11)}$$

$$where\ S < C(1 - \alpha)$$

Where R_a is the actual dam release [$m^3\ s^{-1}$], S the dam storage capacity [m^3], α the fraction of the capacity that is the desired maximum [-], β the exponent determining the correction increase [-] and γ the parameter determining the period when the release is corrected [s^{-1}]. In testing the exponent and period were tuned to 0.6 and 5 days respectively.

6.4 Appendix D: Water demand

6.4.1 Fitting and validation data

Data on irrigation, domestic and industrial water withdrawals were based on the AQUASTAT database (FAO, 2016), EUROSTAT database (EC, 2019) and United Nations World Water Development Report (Connor, 2015). Data on GDP per capita and GVA was abstracted from the Maddison Project Database 2018 (Bolt et al., 2018), Penn World Table 9.0 (Feenstra et al., 2015) and World Bank Development Indicators (World bank, 2010).

Available data for domestic an industrial withdrawals were divided into a dataset used for parameter fitting (80 %) and a dataset used for validation (20 %). Domestic water demands were estimated for each United Nations sub-region, and thus data was divided per sub-region to ensure a good global coverage of data. In the same manner industrial water demand were divided per country. In case there is only a single data point, the data was added to both the fitting and validation data.

6.4.2 Irrigation sector

Conventional irrigation demands were calculated when soil moisture contents drop below the critical threshold where evapotranspiration will be limited. Demands were set to relieve water stress (Eq. A.12). Paddy irrigation demands were set to always keep the soil moisture content of the upper soil layer saturated (Eq. A.13), similar to Hanasaki et al. (2008b) and Wada et al. (2014). For paddy irrigation, the saturated hydraulic conductivity of the upper soil layer was reduced by its cubed root to simulate puddling practices, as recommended by the CROPWAT model (Smith, 1996). Total irrigation demands were adjusted by the irrigation efficiency (Eq. A.14). Paddy irrigation used an irrigation efficiency of 1 since the water losses were already incorporated in the water demand calculation.

$$ID'_{conventional} = (W_{cr,1} + W_{cr,2}) - (W_1 + W_2) \quad \text{Eq. (A.12)}$$

$$where\ W_1 + W_2 < W_{cr,1} + W_{cr,2}$$

$$ID'_{paddy} = W_{max,1} - W_1 \quad \text{Eq. (A.13)}$$

$$where\ W_1 < W_{max,1}$$

$$ID = ID' * IE \quad \text{Eq. (A.14)}$$

Where $ID'_{conventional}$ is the conventional crop irrigation demand [mm], ID'_{paddy} is the paddy crop irrigation demand [mm], ID is the total irrigation demand [mm], W_1 and W_2 are the soil moisture contents of the first and second soil layer respectively [mm], W_{cr} is the critical soil moisture content [mm], W_{max} the maximum soil moisture content [mm], and IE is the irrigation efficiency [mm mm^{-1}].

6.4.3 Domestic sector

Domestic water demands were represented by using a sigmoid curve for the calculation of structural domestic water demands (Eq.A.15) and a efficiency rate for the calculation of water-use efficiency increases (Eq. A.16). These equations differ slightly from Alcamo et al. (2003) since our study used the base 10 logarithms of GDP and water withdrawals per capita as they provided a better fit.

$$DSW_y = DSW_{min} + (DSW_{max} - DSW_{min}) * \frac{1}{1+e^{-f(GDP_y - o)}} \quad \text{Eq. (A.15)}$$

$$DW_y = 10^{DSW_y} \cdot TE^{y-y_{base}} \quad \text{Eq. (A.16)}$$

Where *DSW* is the yearly structural domestic withdrawal [log10 m^3 cap^{-1}], *DW* the yearly domestic withdrawal [m^3 cap^{-1}], DW_{min} the minimum structural domestic withdrawal [log10 m^3 cap^{-1}], DW_{max} the maximum structural domestic withdrawal (without technological improvement) [log10 m^3 cap^{-1}], *GDP* the yearly gross domestic product [log10 $USD_{equivalent}$ cap^{-1}], *f* [-] and *o* [log10 $USD_{equivalent}$] the parameters that determine the range and steepness of the sigmoid curve, *y* the year index, *TE* the technological efficiency rate [-], and y_{base} the base year (taken to be 1980).

DW_{min} was set at 7.5 l cap^{-1} d^{-1} based on the World Health Organisation standard (Reed and Reed, 2013), DW_{max} was estimated at around 450 l cap^{-1} y^{-1} based on a global curve fit, and *TE* was set at 0.995, 0.99, and 0.98 for developing, transition and developed countries respectively (United Nations development status classification) based on Flörke et al. (2013). Curve parameters f and o were estimated for the 23 United Nations sub-regions based on the GDP per capita and domestic water withdrawal data. In case insufficient data was available to calculate parameters values, regional (4 sub-regions) or global (4 sub-regions) parameter estimates were used.

6.4.4 Industrial sector

Industrial water demands were represented by using a linear formula for the calculation of structural industrial water demands (Eq. A.17) and a efficiency rate for the calculation of water-use efficiency increases (Eq. A.18).

$$ISW_y = ISW_{int} \cdot GVA_y \quad \text{Eq. (A.17)}$$

711 $$IW_y = \mathrm{ISW_y} \cdot TE^{y-y_{base}}$$ Eq. (A.18)

712 Where *ISW* is the yearly structural industrial withdrawal [m^3], IW_{int} the country specific industrial water
713 intensity [m $USD_{equivalent}^{-1}$], *IW* the yearly industrial withdrawal [m^3], *GVA* the yearly gross value added
714 by industry [$USD_{equivalent}$], *y* the year index, y_{base} the base year (taken to be the year when the industrial
715 water intensity is determined), and *TE* the technological efficiency rate [-].

716 TE was set at 0.976 and 1 for OECD and non-OECD countries respectively before the year 1980, 0.976
717 between the years 1980 and 2000 and 0.99 after the year 2000 based on Flörke et al. (2013). Industrial
718 water intensities were estimated for the 246 United Nations countries based on the GVA and industrial
719 water withdrawal data. In case insufficient data was available to calculate the industrial water intensities,
720 either sub-regional (56 countries), regional (17 countries) or global (9 countries) intensities estimates
721 were used.

722 **6.4.5 Energy sector**

723 For each thermoelectric power plant the water intensity was combined with their generation to calculate
724 the water demands (Eq. A.19). Actual generation is estimated by adjusting the installed generation
725 capacity by 46 % for fossil, 72 % for nuclear and 56 % for biomass power plants (based on EIA national
726 annual generation data (EIA, 2013))

727 $$EW_y = EW_{int} \cdot G_y$$ Eq. (A.19)

728 Where *EW* is the yearly energy withdrawal [m^3], EW_{int} the energy water intensity [m^3 MWh^{-1}], *G* the
729 yearly generation for each plant [MWh], and *y* the year index.

730 The energy water demands were subtracted from the industrial water demands at the location of each
731 power plant. In cases where the grid cell industrial water demand was less than the energy water demand,
732 national industrial water demands were lowered. In cases where even the national industrial water
733 demands were less than the national energy water demand (3 countries), the energy water demands were
734 lowered instead. Energy demands were lowered until 10 % of the national industrial water demand
735 remains, to ensure some spatial coverage of industrial and energy water demands.

6.4.6 Livestock sector

Livestock water demands were estimated by combining the livestock population with the water requirements for each livestock variety (Eq. A.20).

$$LW_y = LW_{int} \cdot L \quad \text{Eq. (A.20)}$$

Where LW is the yearly livestock withdrawal [m^3], LW_{int} the livestock water intensity [m^3 $livestock^{-1}$], L the livestock number for each variety [livestock].

6.5 Appendix E: General performance

VIC-WUR monthly discharge and monthly terrestrial total water storage anomalies were compared with observations from the GRDC dataset (GRDC, 2003) and GRACE satellite dataset (NASA, 2002) for eight major river basins (not included in the main text). Discharge stations were selected if the upstream area was larger than 10000 m2, matched the simulated upstream area at the station location,): Amazon, Congo, Lena, Volga, Yangtze, Danube, Columbia and Mississippi river basins. A 300km gaussian filer has been applied to the total water storage simulation data (similar to Long et al. (2015)).

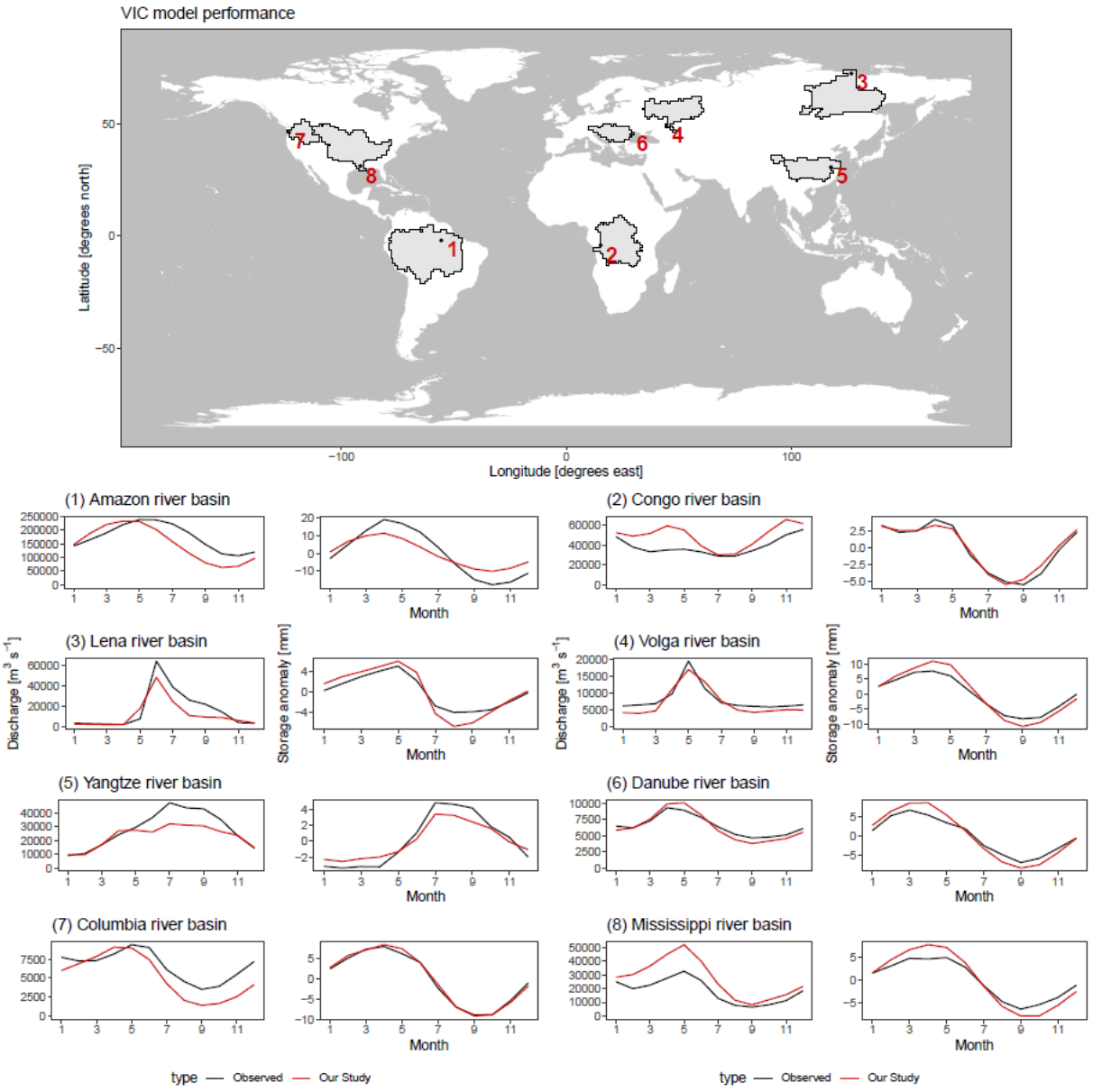

Figure A1: Comparison between simulated and observed discharge and terrestrial total water storage anomalies. Figures indicate multi-year averages of human-impacted simulations (red) and observations (black).

7 Author contribution

Bram Droppers and Wietse H.P. Franssen developed and tested the model additions introduced in VIC-WUR. Bram Droppers generated and analysed the results. Michelle T.H. van Vliet, Bart Nijssen and Fulco Ludwig provided overall oversight and guidance. Bram Droppers prepared the manuscript with contributions from all co-authors.

8 Competing interests

The authors declare that they have no conflict of interest.

9 Acknowledgements

We would like to thank Rik Leemans for his guidance and detailed comments. We would like to thank the Wageningen Institute for Environment and Climate Research (WIMEK) for providing funding for our research.

10 References

Abdulla, F. A., Lettenmaier, D. P., Wood, E. F., and Smith, J. A.: Application of a macroscale hydrologic model to estimate the water balance of the Arkansas Red River basin, J Geophys Res-Atmos, 101, 7449-7459, 10.1029/95jd02416, 1996.

Alcamo, J., Döll, P., Kaspar, F., and Siebert, S.: Global change and global scenarios of water use and availability: an application of WaterGAP1.0, Center for environmental systems research, University of Kassel, Kassel, Germany, 96, 1997.

Alcamo, J., Döll, P., Henrichs, T., Kaspar, F., Lehner, B., Rosch, T., and Siebert, S.: Development and testing of the WaterGAP 2 global model of water use and availability, Hydrolog Sci J, 48, 317-337, 10.1623/hysj.48.3.317.45290, 2003.

Allen, R. G., Pereira, L. S., Raes, D., and Smith, M.: Crop Evapotranspiration - Guidelines for computing crop water requirements, Food and Agricultural Organisation, Rome, Italy, 326, 1998.

Andreadis, K. M., Storck, P., and Lettenmaier, D. P.: Modeling snow accumulation and ablation processes in forested environments, Water Resour Res, 45, 10.1029/2008wr007042, 2009.

Babel, M. S., Das Gupta, A., and Pradhan, P.: A multivariate econometric approach for domestic water demand modeling: An application to Kathmandu, Nepal, Water Resour Manag, 21, 573-589, 10.1007/s11269-006-9030-6, 2007.

Bazilian, M., Rogner, H., Howells, M., Hermann, S., Arent, D., Gielen, D., Steduto, P., Mueller, A., Komor, P., Tol, R. S. J., and Yumkella, K. K.: Considering the energy, water and food nexus: Towards an integrated modelling approach, Energ Policy, 39, 7896-7906, 10.1016/j.enpol.2011.09.039, 2011.

Best, M. J., Pryor, M., Clark, D. B., Rooney, G. G., Essery, R. L. H., Menard, C. B., Edwards, J. M., Hendry, M. A., Porson, A., Gedney, N., Mercado, L. M., Sitch, S., Blyth, E., Boucher, O., Cox, P. M., Grimmond, C. S. B., and Harding, R. J.: The Joint UK Land Environment Simulator

(JULES), model description - Part 1: Energy and water fluxes, Geosci Model Dev, 4, 677-699, 10.5194/gmd-4-677-2011, 2011.

Biemans, H., Haddeland, I., Kabat, P., Ludwig, F., Hutjes, R. W. A., Heinke, J., von Bloh, W., and Gerten, D.: Impact of reservoirs on river discharge and irrigation water supply during the 20th century, Water Resour Res, 47, 10.1029/2009wr008929, 2011.

Bijl, D. L., Bogaart, P. W., Dekker, S. C., and van Vuuren, D. P.: Unpacking the nexus: Different spatial scales for water, food and energy, Global Environ Chang, 48, 22-31, 10.1016/j.gloenvcha.2017.11.005, 2018.

Bolt, J., Inklaar, R., de Jong, H., and van Zanden, J. L.: Rebasing 'Maddison': New income comparisons and the shape of long-run economic developments, University of Groningen, Groningen, the Netherlands, 69, 2018.

Bondeau, A., Smith, P. C., Zaehle, S., Schaphoff, S., Lucht, W., Cramer, W., Gerten, D., Lotze-Campen, H., Muller, C., Reichstein, M., and Smith, B.: Modelling the role of agriculture for the 20th century global terrestrial carbon balance, Global Change Biol, 13, 679-706, 10.1111/j.1365-2486.2006.01305.x, 2007.

Bowling, L. C., Pomeroy, J. W., and Lettenmaier, D. P.: Parameterization of blowing-snow sublimation in a macroscale hydrology model, J Hydrometeorol, 5, 745-762, 10.1175/1525-7541(2004)005<0745:Pobsia>2.0.Co;2, 2004.

Brooks, R. H., and Corey, A. T.: Hydraulic properties of porous media, Colorado state university, Fort Collins, Colorado, 27, 1964.

Brouwer, C., Prins, K., and Heibloem, M.: Irrigation water management: Irrigation scheduling, Food and Agricultural Organisation, Rome, Italy, 66, 1989.

Calder, I. R.: Hydrologic effects of land use change, in: Handbook of hydrology, edited by: Maidment, D. R., McGraw-Hill, New York, 13, 1993.

Carpenter, S. R., Stanley, E. H., and Vander Zanden, M. J.: State of the World's Freshwater Ecosystems: Physical, Chemical, and Biological Changes, Annu Rev Env Resour, 36, 75-99, 10.1146/annurev-environ-021810-094524, 2011.

Carter, A. J., and Scholes, R. J.: Generating a global database of soil properties, IGBP Data and Information Services, Potsdam, Germany, 10, 1999.

Chateau, J., Dellink, R., and Lanzi, E.: An overview of the OECD ENV-linkages model, Organisation for economic co-operation and development, 43, 2014.

Chegwidden, O. S., Nijssen, B., Rupp, D. E., Arnold, J. R., Clark, M. P., Hamman, J. J., Kao, S.-C., Mao, Y., Mizukami, N., Mote, P. W., Pan, M., Pytlak, E., and Xiao, M.: How Do Modeling Decisions Affect the Spread Among Hydrologic Climate Change Projections? Exploring a Large Ensemble of Simulations Across a Diversity of Hydroclimates, Earth's Future, 7, 623-637, 10.1029/2018ef001047, 2019.

824 Cherkauer, K. A., and Lettenmaier, D. P.: Hydrologic effects of frozen soils in the upper Mississippi
825 River basin, J Geophys Res-Atmos, 104, 19599-19610, 10.1029/1999jd900337, 1999.
826 Cherkauer, K. A., and Lettenmaier, D. P.: Simulation of spatial variability in snow and frozen soil, J
827 Geophys Res-Atmos, 108, 10.1029/2003jd003575, 2003.
828 Connor, R.: Water for a sustainable world, United Nations Educational, Scientific and Cultural
829 Organisation, Paris, France, 139, 2015.
830 Cosby, B. J., Hornberger, G. M., Clapp, R. B., and Ginn, T. R.: A Statistical Exploration of the
831 Relationships of Soil-Moisture Characteristics to the Physical-Properties of Soils, Water Resour
832 Res, 20, 682-690, 10.1029/WR020i006p00682, 1984.
833 de Graaf, I. E. M., van Beek, R. L. P. H., Gleeson, T., Moosdorf, N., Schmitz, O., Sutanudjaja, E. H.,
834 and Bierkens, M. F. P.: A global-scale two-layer transient groundwater model: Development
835 and application to groundwater depletion, Adv Water Resour, 102, 53-67,
836 10.1016/j.advwatres.2017.01.011, 2017.
837 Deardorff, J. W.: Efficient Prediction of Ground Surface-Temperature and Moisture, with Inclusion of
838 a Layer of Vegetation, J Geophys Res-Oceans, 83, 1889-1903, 10.1029/JC083iC04p01889,
839 1978.
840 Döll, P., Fiedler, K., and Zhang, J.: Global-scale analysis of river flow alterations due to water
841 withdrawals and reservoirs, Hydrol Earth Syst Sc, 13, 2413-2432, 2009.
842 Döll, P., Hoffmann-Dobrev, H., Portmann, F. T., Siebert, S., Eicker, A., Rodell, M., Strassberg, G., and
843 Scanlon, B. R.: Impact of water withdrawals from groundwater and surface water on continental
844 water storage variations, J Geodyn, 59-60, 143-156, 10.1016/j.jog.2011.05.001, 2012.
845 Döll, P., Müller Schmied, H., Schuh, C., Portmann, F. T., and Eicker, A.: Global-scale assessment of
846 groundwater depletion and related groundwater abstractions: Combining hydrological modeling
847 with information from well observations and GRACE satellites, Water Resour Res, 50, 5698-
848 5720, 10.1002/2014wr015595, 2014.
849 Döll, P., Douville, H., Guntner, A., Muller Schmied, H., and Wada, Y.: Modelling Freshwater Resources
850 at the Global Scale: Challenges and Prospects, Surv Geophys, 37, 195-221, 10.1007/s10712-
851 015-9343-1, 2016.
852 Ducoudre, N. I., Laval, K., and Perrier, A.: Sechiba, a New Set of Parameterizations of the Hydrologic
853 Exchanges at the Land Atmosphere Interface within the Lmd Atmospheric General-Circulation
854 Model, J Climate, 6, 248-273, 10.1175/1520-0442(1993)006<0248:Sansop>2.0.Co;2, 1993.
855 Famiglietti, J. S.: The global groundwater crisis, Nat Clim Change, 4, 945-948, 10.1038/nclimate2425,
856 2014.
857 Feenstra, R. C., Inklaar, R., and Timmer, M. P.: The Next Generation of the Penn World Table, Am
858 Econ Rev, 105, 3150-3182, 10.1257/aer.20130954, 2015.

Flörke, M., and Alcamo, J.: European outlook on water use, Centre for environmental systems research, Kassel, 86, 2004.

Flörke, M., Kynast, E., Barlund, I., Eisner, S., Wimmer, F., and Alcamo, J.: Domestic and industrial water uses of the past 60 years as a mirror of socio-economic development: A global simulation study, Global Environ Chang, 23, 144-156, 10.1016/j.gloenvcha.2012.10.018, 2013.

Franchini, M., and Pacciani, M.: Comparative-Analysis of Several Conceptual Rainfall Runoff Models, J Hydrol, 122, 161-219, 10.1016/0022-1694(91)90178-K, 1991.

Frenken, K., and Gillet, V.: Irrigation water requirement and water withdrawal by country, Food and agricultural organisation, Rome, Italy, 264, 2012.

Gerten, D., Hoff, H., Rockstrom, J., Jagermeyr, J., Kummu, M., and Pastor, A. V.: Towards a revised planetary boundary for consumptive freshwater use: role of environmental flow requirements, Curr Opin Env Sust, 5, 551-558, 10.1016/j.cosust.2013.11.001, 2013.

Gilbert, M., Nicolas, G., Cinardi, G., Van Boeckel, T. P., Vanwambeke, S. O., Wint, G. R. W., and Robinson, T. P.: Global distribution data for cattle, buffaloes, horses, sheep, goats, pigs, chickens and ducks in 2010, Sci Data, 5, 10.1038/sdata.2018.227, 2018.

Gleeson, T., and Richter, B.: How much groundwater can we pump and protect environmental flows through time? Presumptive standards for conjunctive management of aquifers and rivers, River Res Appl, 34, 83-92, 10.1002/rra.3185, 2018.

Gleick, P. H., Cooley, H., Katz, D., Lee, E., Morrison, J., Meena, P., Samulon, A., and Wolff, G. H.: The world's water 2006-2007: The biennial report on freshwater resources, Island Press, Washington, 392 pp., 2013.

Goldewijk, K. K., Beusen, A., Doelman, J., and Stehfest, E.: Anthropogenic land use estimates for the Holocene - HYDE 3.2, Earth Syst Sci Data, 9, 927-953, 10.5194/essd-9-927-2017, 2017.

Goldstein, R., and Smith, W.: U.S. water consumption for power production - the next half century, Electric power research institute, California, United States, 57, 2002.

Grill, G., Lehner, B., Thieme, M., Geenen, B., Tickner, D., Antonelli, F., Babu, S., Borrelli, P., Cheng, L., Crochetiere, H., Macedo, H. E., Filgueiras, R., Goichot, M., Higgins, J., Hogan, Z., Lip, B., McClain, M. E., Meng, J., Mulligan, M., Nilsson, C., Olden, J. D., Opperman, J. J., Petry, P., Liermann, C. R., Saenz, L., Salinas-Rodriguez, S., Schelle, P., Schmitt, R. J. P., Snider, J., Tan, F., Tockner, K., Valdujo, P. H., van Soesbergen, A., and Zarfl, C.: Mapping the world's free-flowing rivers, Nature, 569, 215-+, 10.1038/s41586-019-1111-9, 2019.

Grobicki, A., Huidobro, P., Galloni, S., Asano, T., and Delgau, K. F.: Water, a shared responsibility (chapter 8), United Nations Educational, Scientific and Cultural Organisation, Paris, France, 601, 2005.

Haddeland, I., Lettenmaier, D. P., and Skaugen, T.: Effects of irrigation on the water and energy balances of the Colorado and Mekong river basins, J Hydrol, 324, 210-223, 10.1016/j.jhydrol.2005.09.028, 2006a.

Haddeland, I., Skaugen, T., and Lettenmaier, D. P.: Anthropogenic impacts on continental surface water fluxes, Geophys Res Lett, 33, 10.1029/2006gl026047, 2006b.

Hagemann, S., and Gates, L. D.: Validation of the hydrological cycle of ECMWF and NCEP reanalyses using the MPI hydrological discharge model, J Geophys Res-Atmos, 106, 1503-1510, 10.1029/2000jd900568, 2001.

Hamlet, A. F., and Lettenmaier, D. P.: Effects of climate change on hydrology and water resources in the Columbia River basin, J Am Water Resour As, 35, 1597-1623, DOI 10.1111/j.1752-1688.1999.tb04240.x, 1999.

Hamman, J., Nijssen, B., Brunke, M., Cassano, J., Craig, A., DuVivier, A., Hughes, M., Lettenmaier, D. P., Maslowski, W., Osinski, R., Roberts, A., and Zeng, X. B.: Land Surface Climate in the Regional Arctic System Model, J Climate, 29, 6543-6562, 10.1175/Jcli-D-15-0415.1, 2016.

Hamman, J., Nijssen, B., Roberts, A., Craig, A., Maslowski, W., and Osinski, R.: The coastal streamflow flux in the Regional Arctic System Model, J Geophys Res-Oceans, 122, 1683-1701, 10.1002/2016jc012323, 2017.

Hamman, J. J., Nijssen, B., Bohn, T. J., Gergel, D. R., and Mao, Y. X.: The Variable Infiltration Capacity model version 5 (VIC-5): infrastructure improvements for new applications and reproducibility, Geosci Model Dev, 11, 3481-3496, 10.5194/gmd-11-3481-2018, 2018.

Hanasaki, N., Kanae, S., and Oki, T.: A reservoir operation scheme for global river routing models, J Hydrol, 327, 22-41, 10.1016/j.jhydrol.2005.11.011, 2006.

Hanasaki, N., Kanae, S., Oki, T., Masuda, K., Motoya, K., Shirakawa, N., Shen, Y., and Tanaka, K.: An integrated model for the assessment of global water resources Part 2: Applications and assessments, Hydrol Earth Syst Sc, 12, 1027-1037, 10.5194/hess-12-1027-2008, 2008a.

Hanasaki, N., Kanae, S., Oki, T., Masuda, K., Motoya, K., Shirakawa, N., Shen, Y., and Tanaka, K.: An integrated model for the assessment of global water resources Part 1: Model description and input meteorological forcing, Hydrol Earth Syst Sc, 12, 1007-1025, 10.5194/hess-12-1007-2008, 2008b.

Hanasaki, N., Fujimori, S., Yamamoto, T., Yoshikawa, S., Masaki, Y., Hijioka, Y., Kainuma, M., Kanamori, Y., Masui, T., and Takahashi, K.: A global water scarcity assessment under Shared Socio-economic Pathways–Part 1: Water use, Hydrol Earth Syst Sc, 17, 2375-2391, 2013.

Hanasaki, N., Yoshikawa, S., Pokhrel, Y., and Kanae, S.: A global hydrological simulation to specify the sources of water used by humans, Hydrol Earth Syst Sc, 22, 789-817, 10.5194/hess-22-789-2018, 2018.

928 Hansen, M. C., Defries, R. S., Townshend, J. R. G., and Sohlberg, R.: Global land cover classification
929 at 1km spatial resolution using a classification tree approach, Int J Remote Sens, 21, 1331-1364,
930 Doi 10.1080/014311600210209, 2000.
931 Harding, R., Best, M., Blyth, E., Hagemann, S., Kabat, P., Tallaksen, L. M., Warnaars, T., Wiberg, D.,
932 Weedon, G. P., Lanen, H. v., Ludwig, F., and Haddeland, I.: WATCH: Current Knowledge of
933 the Terrestrial Global Water Cycle, J Hydrometeorol, 12, 1149-1156, 10.1175/jhm-d-11-024.1,
934 2011.
935 Hejazi, M., Edmonds, J., Clarke, L., Kyle, P., Davies, E., Chaturvedi, V., Wise, M., Patel, P., Eom, J.,
936 Calvin, K., Moss, R., and Kim, S.: Long-term global water projections using six socioeconomic
937 scenarios in an integrated assessment modeling framework, Technol Forecast Soc, 81, 205-226,
938 10.1016/j.techfore.2013.05.006, 2014.
939 Huang, Z., Hejazi, M., Li, X., Tang, Q., Vernon, C., Leng, G., Liu, Y., Döll, P., Eisner, S., Gerten, D.,
940 Hanasaki, N., and Wada, Y.: Reconstruction of global gridded monthly sectoral water
941 withdrawals for 1971–2010 and analysis of their spatiotemporal patterns, Hydrol. Earth Syst.
942 Sci., 22, 2117-2133, 10.5194/hess-22-2117-2018, 2018.
943 Jägermeyr, J., Pastor, A., Biemans, H., and Gerten, D.: Reconciling irrigated food production with
944 environmental flows for Sustainable Development Goals implementation, Nature
945 Communications, 8, 15900, 10.1038/ncomms15900, 2017.
946 Kim, S. H., Hejazi, M., Liu, L., Calvin, K., Clarke, L., Edmonds, J., Kyle, P., Patel, P., Wise, M., and
947 Davies, E.: Balancing global water availability and use at basin scale in an integrated assessment
948 model, Climatic Change, 136, 217-231, 10.1007/s10584-016-1604-6, 2016.
949 Konikow, L. F.: Contribution of global groundwater depletion since 1900 to sea-level rise, Geophys Res
950 Lett, 38, 10.1029/2011gl048604, 2011.
951 Krinner, G., Viovy, N., de Noblet-Ducoudre, N., Ogee, J., Polcher, J., Friedlingstein, P., Ciais, P., Sitch,
952 S., and Prentice, I. C.: A dynamic global vegetation model for studies of the coupled atmosphere-
953 biosphere system, Global Biogeochem Cy, 19, 10.1029/2003gb002199, 2005.
954 Lehner, B., Liermann, C. R., Revenga, C., Vorosmarty, C., Fekete, B., Crouzet, P., Döll, P., Endejan,
955 M., Frenken, K., Magome, J., Nilsson, C., Robertson, J. C., Rodel, R., Sindorf, N., and Wisser,
956 D.: High-resolution mapping of the world's reservoirs and dams for sustainable river-flow
957 management, Front Ecol Environ, 9, 494-502, 10.1890/100125, 2011.
958 Liang, X., Lettenmaier, D. P., Wood, E. F., and Burges, S. J.: A Simple Hydrologically Based Model of
959 Land-Surface Water and Energy Fluxes for General-Circulation Models, J Geophys Res-Atmos,
960 99, 14415-14428, 10.1029/94jd00483, 1994.
961 Lohmann, D., NolteHolube, R., and Raschke, E.: A large-scale horizontal routing model to be coupled
962 to land surface parametrization schemes, Tellus A, 48, 708-721, 10.1034/j.1600-0870.1996.t01-
963 3-00009.x, 1996.

964 Lohmann, D., Raschke, E., Nijssen, B., and Lettenmaier, D. P.: Regional scale hydrology: I. Formulation
965 of the VIC-2L model coupled to a routing model, Hydrolog Sci J, 43, 131-141,
966 10.1080/02626669809492107, 1998a.
967 Lohmann, D., Raschke, E., Nijssen, B., and Lettenmaier, D. P.: Regional scale hydrology: II.
968 Application of the VIC-2L model to the Weser River, Germany, Hydrolog Sci J, 43, 143-158,
969 10.1080/02626669809492108, 1998b.
970 Long, D., Yang, Y., Wada, Y., Hong, Y., Liang, W., Chen, Y., Yong, B., Hou, A., Wei, J., and Chen,
971 L.: Deriving scaling factors using a global hydrological model to restore GRACE total water
972 storage changes for China's Yangtze River Basin, Remote Sens Environ, 168, 177-193,
973 10.1016/j.rse.2015.07.003, 2015.
974 Masaki, Y., Hanasaki, N., Takahashi, K., and Hijioka, Y.: Consequences of implementing a reservoir
975 operation algorithm in a global hydrological model under multiple meteorological forcing,
976 Hydrological Sciences Journal, 63, 1047-1061, 10.1080/02626667.2018.1473872, 2018.
977 Mekonnen, M. M., and Hoekstra, A. Y.: Four billion people facing severe water scarcity, Sci Adv, 2,
978 10.1126/sciadv.1500323, 2016.
979 Mo, K. C.: Model-Based Drought Indices over the United States, J Hydrometeorol, 9, 1212-1230,
980 10.1175/2008jhm1002.1, 2008.
981 Myneni, R. B., Nemani, R. R., and Running, S. W.: Estimation of global leaf area index and absorbed
982 par using radiative transfer models, Ieee T Geosci Remote, 35, 1380-1393, 10.1109/36.649788,
983 1997.
984 Nazemi, A., and Wheater, H. S.: On inclusion of water resource management in Earth system models -
985 Part 2: Representation of water supply and allocation and opportunities for improved modeling,
986 Hydrol Earth Syst Sc, 19, 63-90, 10.5194/hess-19-63-2015, 2015a.
987 Nazemi, A., and Wheater, H. S.: On inclusion of water resource management in Earth system models -
988 Part 1: Problem definition and representation of water demand, Hydrol Earth Syst Sc, 19, 33-61,
989 10.5194/hess-19-33-2015, 2015b.
990 Nijssen, B., Lettenmaier, D. P., Liang, X., Wetzel, S. W., and Wood, E. F.: Streamflow simulation for
991 continental-scale river basins, Water Resour Res, 33, 711-724, 10.1029/96wr03517, 1997.
992 Nijssen, B., O'Donnell, G. M., Hamlet, A. F., and Lettenmaier, D. P.: Hydrologic sensitivity of global
993 rivers to climate change, Climatic Change, 50, 143-175, 10.1023/A:1010616428763, 2001a.
994 Nijssen, B., O'Donnell, G. M., Lettenmaier, D. P., Lohmann, D., and Wood, E. F.: Predicting the
995 discharge of global rivers, J Climate, 14, 3307-3323, 10.1175/1520-
996 0442(2001)014<3307:Ptdogr>2.0.Co;2, 2001b.
997 Nijssen, B., Schnur, R., and Lettenmaier, D. P.: Global retrospective estimation of soil moisture using
998 the variable infiltration capacity land surface model, 1980-93, J Climate, 14, 1790-1808,
999 10.1175/1520-0442(2001)014<1790:Greosm>2.0.Co;2, 2001c.

Nilsson, C., Reidy, C. A., Dynesius, M., and Revenga, C.: Fragmentation and flow regulation of the world's large river systems, Science, 308, 405-408, 10.1126/science.1107887, 2005.

Oki, T., Musiake, K., Matsuyama, H., and Masuda, K.: Global Atmospheric Water-Balance and Runoff from Large River Basins, Hydrol Process, 9, 655-678, 10.1002/hyp.3360090513, 1995.

Oki, T., and Kanae, S.: Global hydrological cycles and world water resources, Science, 313, 1068-1072, 10.1126/science.1128845, 2006.

Pastor, A. V., Ludwig, F., Biemans, H., Hoff, H., and Kabat, P.: Accounting for environmental flow requirements in global water assessments, Hydrol Earth Syst Sc, 18, 5041-5059, 10.5194/hess-18-5041-2014, 2014.

Pastor, A. V., Palazzo, A., Havlik, P., Biemans, H., Wada, Y., Obersteiner, M., Kabat, P., and Ludwig, F.: The global nexus of food–trade–water sustaining environmental flows by 2050, Nature Sustainability, 2, 499-507, 10.1038/s41893-019-0287-1, 2019.

Poff, N. L., Richter, B. D., Arthington, A. H., Bunn, S. E., Naiman, R. J., Kendy, E., Acreman, M., Apse, C., Bledsoe, B. P., Freeman, M. C., Henriksen, J., Jacobson, R. B., Kennen, J. G., Merritt, D. M., O'Keeffe, J. H., Olden, J. D., Rogers, K., Tharme, R. E., and Warner, A.: The ecological limits of hydrologic alteration (ELOHA): a new framework for developing regional environmental flow standards, Freshwater Biol, 55, 147-170, 10.1111/j.1365-2427.2009.02204.x, 2010.

Pokhrel, Y., Hanasaki, N., Koirala, S., Cho, J., Yeh, P. J.-F., Kim, H., Kanae, S., and Oki, T.: Incorporating Anthropogenic Water Regulation Modules into a Land Surface Model, J Hydrometeorol, 13, 255-269, 10.1175/jhm-d-11-013.1, 2012a.

Pokhrel, Y., Hanasaki, N., Koirala, S., Cho, J., Yeh, P. J. F., Kim, H., Kanae, S., and Oki, T.: Incorporating Anthropogenic Water Regulation Modules into a Land Surface Model, J Hydrometeorol, 13, 255-269, 10.1175/Jhm-D-11-013.1, 2012b.

Pokhrel, Y. N., Koirala, S., Yeh, P. J.-F., Hanasaki, N., Longuevergne, L., Kanae, S., and Oki, T.: Incorporation of groundwater pumping in a global Land Surface Model with the representation of human impacts, Water Resour Res, 51, 78-96, 10.1002/2014wr015602, 2015.

Pokhrel, Y. N., Hanasaki, N., Wada, Y., and Kim, H.: Recent progresses in incorporating human land-water management into global land surface models toward their integration into Earth system models, Wires Water, 3, 548-574, 10.1002/wat2.1150, 2016.

Portmann, F. T., Siebert, S., and Döll, P.: MIRCA2000-Global monthly irrigated and rainfed crop areas around the year 2000: A new high-resolution data set for agricultural and hydrological modeling, Global Biogeochem Cy, 24, 10.1029/2008gb003435, 2010.

Postel, S. L., Daily, G. C., and Ehrlich, P. R.: Human appropriation of renewable fresh water, Science, 271, 785-788, 10.1126/science.271.5250.785, 1996.

Reed, B., and Reed, B.: How much water is needed in emergencies, Water, Engineering and Development Centre, Leicestershire, 2013.

Richter, B. D., Davis, M. M., Apse, C., and Konrad, C.: A Presumptive Standard for Environmental Flow Protection, River Res Appl, 28, 1312-1321, 10.1002/rra.1511, 2012.

Rodell, M., Velicogna, I., and Famiglietti, J. S.: Satellite-based estimates of groundwater depletion in India, Nature, 460, 999-U980, 10.1038/nature08238, 2009.

Roman, M. O., Wang, Z. S., Sun, Q. S., Kalb, V., Miller, S. D., Molthan, A., Schultz, L., Bell, J., Stokes, E. C., Pandey, B., Seto, K. C., Hall, D., Oda, T., Wolfe, R. E., Lin, G., Golpayegani, N., Devadiga, S., Davidson, C., Sarkar, S., Praderas, C., Schmaltz, J., Boller, R., Stevens, J., Gonzalez, O. M. R., Padilla, E., Alonso, J., Detres, Y., Armstrong, R., Miranda, I., Conte, Y., Marrero, N., MacManus, K., Esch, T., and Masuoka, E. J.: NASA's Black Marble nighttime lights product suite, Remote Sens Environ, 210, 113-143, 10.1016/j.rse.2018.03.017, 2018.

Rost, S., Gerten, D., Bondeau, A., Lucht, W., Rohwer, J., and Schaphoff, S.: Agricultural green and blue water consumption and its influence on the global water system, Water Resour Res, 44, 10.1029/2007wr006331, 2008.

Rougé, C., Reed, P. M., Grogan, D. S., Zuidema, S., Prusevich, A., Glidden, S., Lamontagne, J. R., and Lammers, R. B.: Coordination and Control: Limits in Standard Representations of Multi-Reservoir Operations in Hydrological Modeling, Hydrol. Earth Syst. Sci. Discuss., 2019, 1-37, 10.5194/hess-2019-589, 2019.

Sellers, P. J., Tucker, C. J., Collatz, G. J., Los, S. O., Justice, C. O., Dazlich, D. A., and Randall, D. A.: A Global 1-Degrees-by-1-Degrees Ndvi Data Set for Climate Studies .2. The Generation of Global Fields of Terrestrial Biophysical Parameters from the Ndvi, Int J Remote Sens, 15, 3519-3545, 10.1080/01431169408954343, 1994.

Shen, Y., Oki, T., Utsumi, N., Kanae, S., and Hanasaki, N.: Projection of future world water resources under SRES scenarios: water withdrawal/Projection des ressources en eau mondiales futures selon les scénarios du RSSE: prélèvement d'eau, Hydrological sciences journal, 53, 11-33, 2008.

Shiklomanov, I. A.: Appraisal and assessment of world water resources, Water Int, 25, 11-32, Doi 10.1080/02508060008686794, 2000.

Shuttleworth, W. J.: Evaporation, in: Handbook of hydrology, edited by: Maidment, D. R., McGraw-Hill, New York, 53, 1993.

Smakhtin, V., Revenga, C., and Döll, P.: A pilot global assessment of environmental water requirements and scarcity, Water Int, 29, 307-317, 10.1080/02508060408691785, 2004.

Smith, M.: CROPWAT: A computer program for irrigation planning and managemetn, Food and Agricultural Organisation, Rome, Italy, 127, 1996.

Steinfeld, H., Gerber, P., Wassenaar, T. D., Castel, V., Rosales, M., and De Haan, C.: Livestock's long shadow: environmental issues and options, Food and Agricultural Organisation, Rome, Italy, 416 pp., 2006.

Sutanudjaja, E. H., van Beek, R., Wanders, N., Wada, Y., Bosmans, J. H. C., Drost, N., van der Ent, R. J., de Graarf, I. E. M., Hoch, J. M., de Jong, K., Karssenberg, D., Lopez, P. L., Pessenteiner, S., Schmitz, O., Straatsma, M. W., Vannametee, E., Wisser, D., and Bierkens, M. F. P.: PCR-GLOBWB 2: a 5 arcmin global hydrological and water resources model, Geosci Model Dev, 11, 2429-2453, 10.5194/gmd-11-2429-2018, 2018.

Takata, K., Emori, S., and Watanabe, T.: Development of the minimal advanced treatments of surface interaction and runoff, Global Planet Change, 38, 209-222, 10.1016/S0921-8181(03)00030-4, 2003.

Tessler, Z. D., Vorosmarty, C. J., Grossberg, M., Gladkova, I., Aizenman, H., Syvitski, J. P. M., and Foufoula-Georgiou, E.: Profiling risk and sustainability in coastal deltas of the world, Science, 349, 638-643, 10.1126/science.aab3574, 2015.

Turner, S. W. D., Hejazi, M., Yonkofski, C., Kim, S. H., and Kyle, P.: Influence of Groundwater Extraction Costs and Resource Depletion Limits on Simulated Global Nonrenewable Water Withdrawals Over the Twenty-First Century, Earth's Future, 7, 123-135, 10.1029/2018ef001105, 2019.

Van Beek, L. P. H., and Bierkens, M. F. P.: The global hydrological model PCR-GLOBWB: conceptualization, parameterization and verification, Departement of physical geography, Utrecht university, Utrecht, The Netherlands, 53, 2008.

van Vliet, M. T. H., Wiberg, D., Leduc, S., and Riahi, K.: Power-generation system vulnerability and adaptation to changes in climate and water resources, Nat Clim Change, 6, 375-+, 10.1038/Nclimate2903, 2016.

Vassolo, S., and Döll, P.: Global-scale gridded estimates of thermoelectric power and manufacturing water use, Water Resour Res, 41, 10.1029/2004wr003360, 2005.

Voisin, N., Li, H., Ward, D., Huang, M., Wigmosta, M., and Leung, L.: On an improved sub-regional water resources management representation for integration into earth system models, Hydrology & Earth System Sciences, 17, 2013a.

Voisin, N., Li, H., Ward, D., Huang, M., Wigmosta, M., and Leung, L. R.: On an improved sub-regional water resources management representation for integration into earth system models, Hydrol Earth Syst Sc, 17, 3605-3622, 10.5194/hess-17-3605-2013, 2013b.

Voisin, N., Hejazi, M. I., Leung, L. R., Liu, L., Huang, M. Y., Li, H. Y., and Tesfa, T.: Effects of spatially distributed sectoral water management on the redistribution of water resources in an integrated water model, Water Resour Res, 53, 4253-4270, 10.1002/2016wr019767, 2017.

Voisin, N., Kintner-Meyer, M., Wu, D., Skaggs, R., Fu, T., Zhou, T., Nguyen, T., and Kraucunas, I.: OPPORTUNITIES FOR JOINT WATER-ENERGY MANAGEMENT Sensitivity of the 2010 Western US Electricity Grid Operations to Climate Oscillations, B Am Meteorol Soc, 99, 299-312, 10.1175/Bams-D-16-0253.1, 2018.

Vorosmarty, C. J., McIntyre, P. B., Gessner, M. O., Dudgeon, D., Prusevich, A., Green, P., Glidden, S., Bunn, S. E., Sullivan, C. A., Liermann, C. R., and Davies, P. M.: Global threats to human water security and river biodiversity, Nature, 467, 555-561, 10.1038/nature09440, 2010.

Voß, F., and Flörke, M.: Spatially explicit estimates of past and present manufacturing and energy water use, Center for environmental systems research, Kassel, 17, 2010.

Wada, Y., van Beek, L. P. H., and Bierkens, M. F. P.: Modelling global water stress of the recent past: on the relative importance of trends in water demand and climate variability, Hydrol Earth Syst Sc, 15, 3785-3808, 10.5194/hess-15-3785-2011, 2011a.

Wada, Y., van Beek, L. P. H., Viviroli, D., Durr, H. H., Weingartner, R., and Bierkens, M. F. P.: Global monthly water stress: 2. Water demand and severity of water stress, Water Resour Res, 47, 10.1029/2010wr009792, 2011b.

Wada, Y., and Bierkens, M. F. P.: Sustainability of global water use: past reconstruction and future projections, Environ Res Lett, 9, 104003, 10.1088/1748-9326/9/10/104003, 2014.

Wada, Y., Wisser, D., and Bierkens, M. F. P.: Global modeling of withdrawal, allocation and consumptive use of surface water and groundwater resources, Earth Syst Dynam, 5, 15-40, 10.5194/esd-5-15-2014, 2014.

Weedon, G. P., Balsamo, G., Bellouin, N., Gomes, S., Best, M. J., and Viterbo, P.: The WFDEI meteorological forcing data set: WATCH Forcing Data methodology applied to ERA-Interim reanalysis data, Water Resour Res, 50, 7505-7514, 10.1002/2014wr015638, 2014.

Wisser, D., Fekete, B. M., Vorosmarty, C. J., and Schumann, A. H.: Reconstructing 20th century global hydrography: a contribution to the Global Terrestrial Network- Hydrology (GTN-H), Hydrol Earth Syst Sc, 14, 1-24, 10.5194/hess-14-1-2010, 2010a.

Wisser, D., Fekete, B. M., Vörösmarty, C. J., and Schumann, A. H.: Reconstructing 20th century global hydrography: a contribution to the Global Terrestrial Network- Hydrology (GTN-H), Hydrol. Earth Syst. Sci., 14, 1-24, 10.5194/hess-14-1-2010, 2010b.

Wood, A. W., and Lettenmaier, D. P.: A test bed for new seasonal hydrologic forecasting approaches in the western United States, B Am Meteorol Soc, 87, 1699-+, 10.1175/Bams-87-12-1699, 2006.

Yassin, F., Razavi, S., Elshamy, M., Davison, B., Sapriza-Azuri, G., and Wheater, H.: Representation and improved parameterization of reservoir operation in hydrological and land-surface models, Hydrol. Earth Syst. Sci., 23, 3735-3764, 10.5194/hess-23-3735-2019, 2019.

Zhao, G., Gao, H. L., Naz, B. S., Kao, S. C., and Voisin, N.: Integrating a reservoir regulation scheme into a spatially distributed hydrological model, Adv Water Resour, 98, 16-31, 10.1016/j.advwatres.2016.10.014, 2016.

Zhou, T., Haddeland, I., Nijssen, B., and Lettenmaier, D. P.: Human induced changes in the global water cycle, AGU Geophysical Monograph Series, Submitted, 2015.

Zhou, T., Nijssen, B., Gao, H. L., and Lettenmaier, D. P.: The Contribution of Reservoirs to Global Land Surface Water Storage Variations, J Hydrometeorol, 17, 309-325, 10.1175/Jhm-D-15-0002.1, 2016.

Zhou, T., Voisin, N., Leng, G. Y., Huang, M. Y., and Kraucunas, I.: Sensitivity of Regulated Flow Regimes to Climate Change in the Western United States, J Hydrometeorol, 19, 499-515, 10.1175/Jhm-D-17-0095.1, 2018.

Zhu, C. M., Leung, L. R., Gochis, D., Qian, Y., and Lettenmaier, D. P.: Evaluating the Influence of Antecedent Soil Moisture on Variability of the North American Monsoon Precipitation in the Coupled MM5/VIC Modeling System, J Adv Model Earth Sy, 1, 10.3894/James.2009.1.13, 2009.